

5. RADIOLARIAN FAUNAL CHARACTERISTICS IN OLIGOCENE SEDIMENTS OF THE KERGUELEN PLATEAU, LEG 183, SITE 1138¹

Marcus Apel,² Wolfgang Kiessling,^{2,3} Florian Böhm,⁴ and David Lazarus²

ABSTRACT

Three sites from Ocean Drilling Program (ODP) Leg 183 (Kerguelen Plateau) have been analyzed to document faunal change in high-latitude radiolarians and to compare the faunal change to Eocene–Oligocene climatic deterioration. Radiolarians are not preserved in Eocene sediments. In Oligocene sediments, radiolarian preservation improves in a stepwise manner toward the Miocene. A total of 115 species were found in lower Oligocene samples from Site 1138; all are documented herein. Radiolarian preservation is presumably linked to productivity triggered by climatic cooling during the early Oligocene. Similar patterns of improving preservation through the Eocene/Oligocene boundary are documented from several Deep Sea Drilling Project and ODP sites in the Southern Ocean, indicating a general pattern. In contrast to the Southern Kerguelen Plateau, however, proxies for productivity are more divergent at Site 1138 (Central Kerguelen Plateau). Whereas carbonate dissolution, as indicated by poor preservation of foraminifers and common hiatuses, is very pronounced in the upper Eocene–lowermost Oligocene, the quality of radiolarian and diatom preservation does not significantly increase until the uppermost lower Oligocene. Multiple measures of radiolarian diversity in the Oligocene from Site 1138 closely parallel radiolarian preservation, indicating that preserved radiolarian diversity is controlled by productivity.

¹Apel, M., Kiessling, W., Böhm, F., and Lazarus, D., 2002. Radiolarian faunal characteristics in Oligocene sediments of the Kerguelen Plateau, Leg 183, Site 1138. *In* Frey, F.A., Coffin, M.F., Wallace, P.J., and Quilty, P.G. (Eds.), *Proc. ODP, Sci. Results*, 183, 1–48 [Online]. Available from World Wide Web: <http://www-odp.tamu.edu/publications/183_SR/VOLUME/CHAPTERS/002.PDF>. [Cited YYYY-MM-DD]

²Humboldt-Universität Berlin, Institut für Paläontologie, Museum für Naturkunde, Invalidenstrasse 43, 10115 Berlin, Germany.

Correspondence author:
marcus.apel@rz.hu-berlin.de

³University of Chicago, Dept. of Geophysical Science, 5734 South Ellis Avenue, Chicago IL, 60637, USA.

⁴GEOMAR, Forschungszentrum für Marine Geowissenschaften, Wischhofstrasse, 1-3, D-24148 Kiel, Germany.

Initial receipt: 14 June 2001

Acceptance: 16 May 2002

Web publication: 18 October 2002

Ms 183SR-002

INTRODUCTION

The role of the Eocene–Oligocene transition in Cenozoic radiolarian evolution is still insufficiently known, especially when compared to that for other microplankton groups such as planktonic foraminifers and calcareous nannoplankton. Some faunal change has been observed in low latitudes (Riedel and Sanfilippo, 1986; Sanfilippo et al., 1985), but it appears minor in comparison to the severe taxonomic turnover reported in planktonic foraminifers (Keller et al., 1992) and calcareous nannoplankton (Aubry, 1992). The climatic deteriorations around the Eocene/Oligocene boundary usually play a major role in the scenarios explaining plankton changes in the Southern Ocean. Most commonly, changes are attributed to an increase in productivity (Baldauf, 1992; Baldauf and Barron, 1990; Diester-Haass, 1995), eventually favoring opal preservation and promoting carbonate dissolution.

As part of a larger project concerning radiolarian faunal change, the original aim of this study was to document the radiolarian faunal change during the late Eocene to the early Oligocene in the Southern Ocean in relation to the outstanding climate change during this time period. Previous studies were devoted mostly to developing a stratigraphic zonation (Caulet, 1991; Takemura, 1992; Takemura and Ling, 1997) but did not characterize overall faunal change in relation to Southern Ocean cooling (Zachos et al., 1999). So far, this has only been done by Lazarus and Caulet (1993), who reported a considerable faunal turnover.

Unfortunately, no radiolarians of Eocene age are preserved in any of the studied sites. Thus, our study is limited to the Oligocene suite and can only document faunal changes within this interval. We document qualitative and quantitative radiolarian faunal characteristics through a large part of the Oligocene and relate this to published paleoclimatic and productivity data. Taxonomy, stratigraphy, diversity, abundance, and preservation of radiolarians are described. A significant accomplishment of this study is the documentation, albeit preliminary, of the complete recovered Oligocene radiolarian assemblage, including (in open nomenclature) several previously undescribed species.

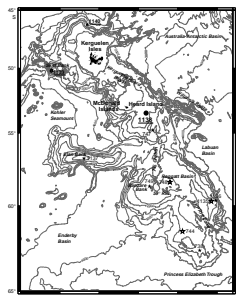
SAMPLES AND METHODS

During Ocean Drilling Program (ODP) Leg 183, the Eocene/Oligocene boundary interval was drilled four times (Table T1). Samples from three sites (1138, 1139, and 1140) (Fig. F1) were studied and, according to shipboard stratigraphic results, contain a sedimentary record of the Eocene/Oligocene boundary. A total of 64 samples were studied for this paper.

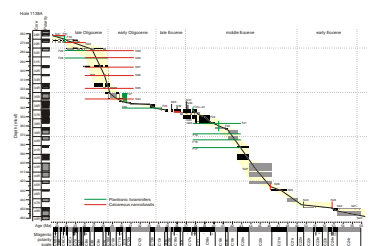
Only Hole 1138A (53°33.105'S, 75°58.493'E; Central Kerguelen Plateau) yielded a good radiolarian record within the time interval of interest, and, even at this site, only Oligocene radiolarians could be identified. The interval is situated within lithofacies Unit III as identified by the Shipboard Scientific Party (2000). This unit ranges in age from about mid-Campanian to late Oligocene and consists of white to light gray and light greenish gray foraminifer-bearing nanofossil chalk. According to the current age model (Fig. F2), the Eocene–Oligocene time period is represented in Cores 183-1138A-29R through 48R. The base of the cored interval for Core 183-1138A-36R (top of Chron C13r) is interpreted as the Eocene/Oligocene boundary,

F1. General data of Leg 183 sites, p. 31.

F1. Kerguelen Plateau and Leg 183 sites, p. 22.



F2. Age-depth plot, Hole 1138A, p. 23.



but there is no core recovery. As indicated by calcareous nannoplankton and paleomagnetic studies, a hiatus or condensed section is present close to the Eocene/Oligocene boundary (Shipboard Scientific Party, 2000). Glauconite-filled foraminifers in Core 183-1138A-36R are further evidence for stratigraphic condensation. No radiolarians were found below Core 183-1138A-36R (Fig. F3). The oldest poorly preserved radiolarians are observed in Sample 183-1138A-36R-1, 41–43 cm (Chron C11r; early Oligocene; ~30.2 Ma). Preservation gradually improves upward through Core 183-1138A-35R and is generally good in Core 183-1138A-34R.

At Site 1139, 15 samples from the upper Eocene–lower Oligocene (Sections 183-1139A-38R-2 to 41R-1) do not contain identifiable radiolarians (Fig. F4). The radiolarian record starts in the uppermost Oligocene (Core 183-1139A-19R), and well-preserved faunas are identified (Cores 183-1139A-17R and 18R) only in the lower Miocene.

Eight samples of early Oligocene to early Miocene age were studied from Site 1140. Oligocene samples are barren of radiolarians. Samples from Site 1140 of early Miocene age had well-preserved faunas in Core 183-1140A-14R. The faunas are dominated by spumellarians with abundant Actinommidae, Litheliidae, and Pyloniidae. Common nassellarians are Artostrobiidae and Plagiacanthidae (Fig. F5).

All material was cleaned with hot hydrochloric acid and H₂O₂ and then was wet sieved (38- μ m mesh). After short ultrasonic treatment, the samples were neutralized with distilled water. The radiolarian slides were prepared by following standard procedures for random grain distribution (Moore, 1973), including an improved coverslip holder for preparing microslides (Lazarus, 1994). The dry SiO₂ material was then embedded in Canada balsam and dried at 60°C. The radiolarian slides were examined with a transmitted light microscope. Pictures were captured directly from this microscope using a high-resolution black-and-white video camera connected to a computer. All images were transferred to a species-oriented image database (Cumulus, Canto Software) for further analysis.

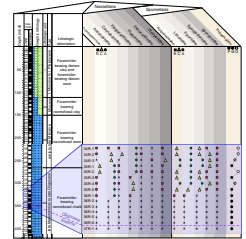
Species counts were based on >400 specimens whenever possible. If <400 specimens were found on the slide, the total slide was counted. Radiolarians were counted along random transects of the slides. Presence/absence data for the biostratigraphic analysis are based on examination of larger portions of the slides than used for the species counts. Total radiolarian abundance was determined on the counts of radiolarians, including fragments. Abundance data are reported as numbers of individuals per gram of dry bulk sediment (except for a rough evaluation of family data) (Figs. F3, F4, F5) rather than our usual interval (Abundant [A], Common [C], Rare [R]) classification.

Preservation of radiolarians was evaluated as follows:

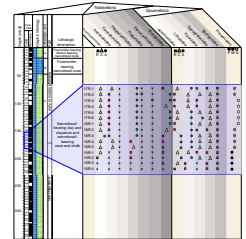
- Poor = <10%,
- Poor to moderate = 10%–30%,
- Moderate = 30%–50%,
- Moderate to good = 50%–70%, and
- Good = >70% of the radiolarians can be identified to the genus level.

In addition, we suggest a new approach to evaluating radiolarian preservation. We tentatively use the relative abundance of robust nassellarians (*Siphocampe* and *Artostrobos*) as an indicator of preservation.

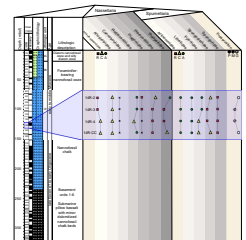
F3. Family level faunal characteristics, Site 1138, p. 25.



F4. Family level faunal characteristics, Site 1139, p. 26.



F5. Family level faunal characteristics, Site 1140, p. 27.



The percentage of diatoms was determined on the counts of all radiolarian fragments and all diatom fragments. A minimum of 10% of the siliceous tests of single specimens had to be preserved to be included in the counts.

Radiolarian diversity was assessed in several ways based on species counts from random views of the radiolarian slides. Other than species richness, diversity has been evaluated by the following criteria:

1. The Shannon index: $H' = -\sum (P_i \times \ln P_i)$, where P_i is the fraction of the i_{th} species of the total fauna. This index provides a rough measure of diversity, which is much less biased by sample size than species richness.
2. Evenness: $J' = H'/H'_{max}$, where H' is the Shannon index as defined above, $H'_{max} = \ln S$, and S is the number of species observed. This index determines how evenly the proportions of taxa are distributed in a sample.
3. Margalef's index: $SR = (S - 1)/\ln N$, where N is the number of individuals. This index provides a measure of species richness that is roughly normalized for sample size without using more complex rarefaction techniques.

Additional faunal indices with a potential paleoceanographic signal are nassellarian/spumellarian ratios, measured as the percentage of spumellarians in the total radiolarian fauna, and the radiolarian/diatom ratio, measured as the percentage of diatoms in the whole siliceous microfauna. Statistical tests were carried out using the statistical software package, SPSS 9.0. Radiolarian slides are curated at the Museum für Naturkunde in Berlin (Germany).

RADIOLARIANS AND DIATOMS AT SITE 1138

A total of 120 radiolarian species were recorded in the samples from Hole 1138A, as summarized in Table T2. A full documentation of the taxonomy of recovered radiolarians is given in "Appendix," p. 16, and in Plates P1, P2, P3, P4, P5, P6, P7, P8, P9, P10.

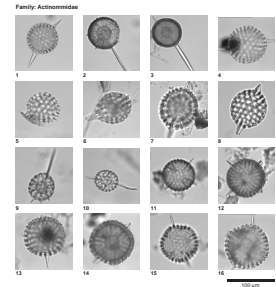
Core 183-1138A-34R

Radiolarians are abundant and usually well preserved in Sections 183-1138A-34R-1 through 34R-3. Sporadically, an abundant diatom flora is present. Diatoms dominate the siliceous microfossil assemblage in Sample 183-1138A-34R-3, 20–22 cm. Stratigraphic markers are present (e.g., *Axoprunum irregularis*, *Lychnocanoma conica*, *Amphistylus?* sp. sensu Takemura, 1992) but are only moderately preserved and rare. Even the relatively well preserved samples of Sections 183-1138A-34R-1 through 34R-3 are dominated by fragmented radiolarians and diatoms rather than by complete specimens.

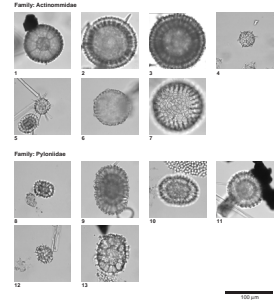
The high abundance of Litheliidae in all samples of Sections 183-1138A-34R-3 through 34R-1 is remarkable. *Lithelius* sp. A gr. (Pl. P3, figs. 1–4), *Lithelius* sp. C (Pl. P3, fig. 6), *Lithelius* sp. D (Pl. P3, fig. 7), and Pylonid sp. 1 (Pl. P2, fig. 8) are common throughout. Spumellaria generally dominate the radiolarian assemblage. Among the nassellarians, Artostrobiidae are the most abundant family, and within the Artostrobiidae, *Siphocampe* and *Artostrobos* dominate. In all samples of Sections 183-1138A-34R-3 through 34R-1, *Siphocampe* and *Artostrobos* are the

T2. Abundance data for all early Oligocene-aged radiolarians, Hole 1138A, p. 32.

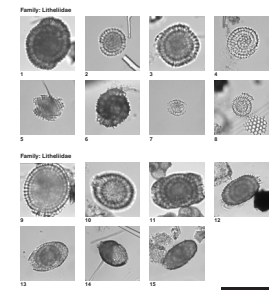
P1. Actinommidae, p. 39.



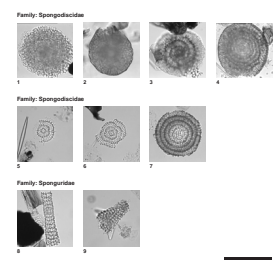
P2. Actinommidae and Pyloniidae, p. 40.



P3. Litheliidae, p. 41.



P4. Spongodiscidae and Sponguroidae, p. 42.



dominant nassellarian genus, and *Artostrobos pusillum* gr. is the most frequent species (Pl. P9, figs. 6–10).

Core 183-1138A-35R

Radiolarians are generally rare to common and poorly to moderately preserved in Core 183-1138A-35R. Stratigraphic markers are present (e.g., *A. irregularis*, *L. conica*, *Amphistylus?* sp. sensu Takemura, 1992, and *Eucyrtidium spinosum*). Spumellarians in general and Litheliidae in particular dominate the assemblages in this interval. *Lithelius* sp. A (Pl. P3, figs. 1–4), *Lithelius* sp. C (Pl. P3, fig. 6), *Lithelius* sp. D (Pl. P3, fig. 7), and Pylonid sp. 1 (Pl. P2, fig. 8) are especially conspicuous. Additional common spumellarians are Actinommidae, especially *Cenosphaera* sp. A gr. (Pl. P2, figs. 6–7), *Amphistylus?* sp. A (Pl. P1, fig. 2), *Actinomma henningmoeni* (Pl. P2, fig. 1), and *Stylosphaera radiosa* gr. (Pl. P1, figs. 6–8). Among the nassellarians, *Siphocampe* and *Artostrobos* are most common, particularly *A. pusillum* (Pl. P9, figs. 6–10), *Siphocampe nodosaria* (Pl. P9, fig. 11), *Siphocampe acephala* gr. (Pl. P9, figs. 14–17), and *Siphocampe arachnea* gr. (Pl. P9, figs. 12, 13). *Peridium?* sp. A and *Peridium?* sp. B (Pl. P5, figs. 18, 19) are generally abundant in these samples except for the two levels at which diversity declines (see below).

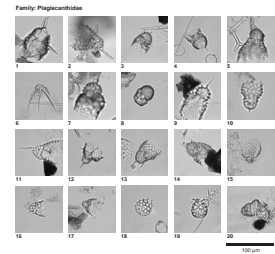
The overall radiolarian diversity is generally lower than that found in Sections 183-1138A-34R-1 through 34R-3. The highest diversity in Core 183-1138A-35R is found in Samples 183-1138A-35R-2, 105–107 cm, and 35R-2, 24–26 cm. There is a conspicuous diversity decline in Sample 183-1138A-35R-1, 140–142 cm, where the assemblage is dominated by Litheliidae. Another diversity drop is observed in Sample 183-1138A-35R-3, 101–103 cm, where Artostrobiidae and Litheliidae dominate the poorly to moderately preserved fauna. Diatoms are common to abundant in this core (Table T3), but diatom diversity is remarkably lower than in Sections 183-1138A-34R-1 through 34R-3.

Stratigraphic markers are present but rare. *A. irregularis* was observed in Samples 183-1138A-35R-5, 51–53 cm; 35R-4 (all); 35R-3, 101–103 cm; 35R-2 (all) to 34R-3 (all); 34R-2, 23–25 cm; and Section 34R-1 (Table T2). *E. spinosum* is present only in Sample 183-1138A-35R-1, 103–105 cm (Table T2). *L. conica* is present in all samples of Section 183-1138A-35R-4; in Samples 183-1138A-35R-2, 105–107 cm, and 35R-1, 140–142 cm; all samples of Section 183-1138A-34R-3; and in Sample 183-1138A-34R-1, 103–105 cm (Table T2).

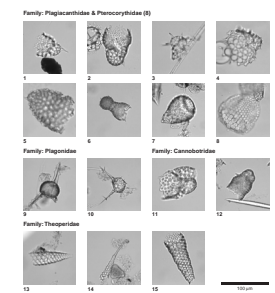
Core 183-1138A-36R

Radiolarians are rare and poorly preserved in Samples 183-1138A-36R-1, 0–2 cm, through 36R-1, 41–43 cm. Almost exclusively, radiolarian fragments rather than complete specimens were observed. Artostrobiidae are dominant, and some additional Actinommidae are present, which contribute most to the observed diversity. Although there is a continuous trend toward declining diversities downcore in Section 183-1138A-36R-1, the very top of the section is characterized by a profound diversity decline. Below interval 183-1138A-36R-1, 40–42 cm, samples are barren of radiolarians. Diatoms are generally rare in all samples of Core 183-1138A-36R.

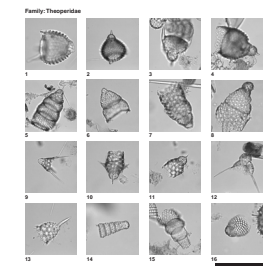
P5. Plagiacanthidae, p. 43.



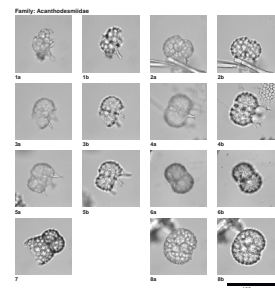
P6. Plagiacanthidae, Pterocorythidae, Plagonidae, Cannobotriidae, and Theoperidae, p. 44.



P7. Theoperidae, p. 45.



P8. Acanthodesmiidae, p. 46.



STRATIGRAPHY

The current age model based on paleomagnetic reversals, planktonic foraminifers, and nannofossil biostratigraphy (Fig. F2), suggests that the radiolarian-bearing Paleogene samples of Site 1138 are of middle early Oligocene to late early Oligocene age (Fig. F6). Owing to a great degree of endemism (Lazarus and Caulet, 1993), direct correlation of recently established Paleogene radiolarian zones of the Southern Ocean (Takemura and Ling, 1997) with lower-latitude chronozones is not possible at a fine scale. Furthermore, the heterogeneous preservation does not allow a straightforward application of Takemura and Ling's (1997) zonation.

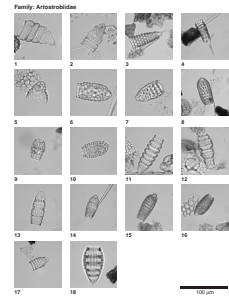
The age-depth model (Fig. F2) interprets the magnetic reversal in Section 183-1138A-36R-1 as the C11r/C11n boundary. The upper 50 cm of Core 183-1138A-36R is thus assigned to Chron C11n. According to the number of magnetic reversals and nannoplankton data, the top of our section in Core 183-1138A-34R should be assigned to Chron C10n.

Only a few radiolarian marker taxa help to constrain the age of our samples, and they give equivocal results, especially compared to the paleomagnetic data. *A. irregularis*, the zonal marker for the *A.?* *irregularis* Zone of Takemura and Ling (1997), is found more or less regularly from Samples 183-1138A-35R-5, 20–22 cm, to 34R-1, 103–105 cm. The vertical distribution of this species agrees well with the age-depth model, indicating a late early Oligocene age. However, *Amphistylus?* sp. sensu Takemura (1992) (= our *Amphistylus?* sp. A) is found in most samples of Cores 183-1138A-34R to 35R, which are placed in Chron C10n to C10r (Fig. F2). This species was previously thought to disappear shortly after the first appearance datum (FAD) of *A. irregularis*, presumably within Chron C12r or earlier, according to Takemura and Ling (1997).

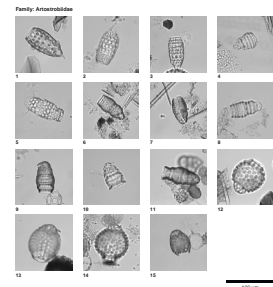
E. spinosum, the zonal marker of the *E. spinosum* Zone, is recorded in Sample 183-1138A-35R-1, 103–105 cm, assigned to Chron C10n (Fig. F2). Based on preliminary paleomagnetic calibrations, Takemura and Ling (1997) gave a range for the last appearance of *E. spinosum* between Chrons C11r and C13n. Further complicating the issue is the first appearance of *L. conica* in Sample 183-1138A-35R-4, 103–105 cm. This species is supposed to appear first in Chrons C11 or C12 (Takemura and Ling, 1997), but its first appearance is assigned to C10r in Hole 1138A (Fig. F2). Other stratigraphic markers of Takemura and Ling (1997) could not be found.

The combination of these somewhat equivocal radiolarian data, the shipboard calcareous nannofossil and foraminifer dates (Shipboard Scientific Party, 2000), and the paleomagnetic results render it likely that some identified radiolarian ranges need to be revised. The revision affects both the absolute ranges and the relative ranges. First, the stratigraphic overlap between *Amphistylus?* sp. and *A. irregularis* is likely to be greater than previously believed. The most parsimonious explanation is that *Amphistylus?* sp. has a later last appearance datum (LAD) than previously believed. Second, *E. spinosum* ranges significantly longer into the Oligocene than implied by Takemura and Ling (1997). Although Takemura (1992) reported finding *E. spinosum* in samples as young as ours, he interpreted those occurrences as reworked. However, we found complete specimens of *E. spinosum* in a well-preserved assemblage; hence, we interpret the occurrence as in situ. Even with the adjustments, the interpretation of the paleomagnetic data, based on radiolarians, is hardly compatible with the interpretations based on calcareous

P9. Artostrobiidae, p. 47.

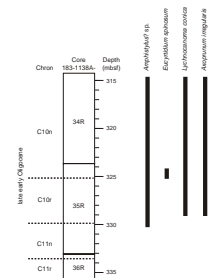


P10. Artostrobiidae from the Kerguelen Plateau, p. 48.



T3. Summary of radiolarian faunal indices, Hole 1138A, p. 37.

F6. Oligocene radiolarian marker taxa, Hole 1138A, p. 28.



nannoplankton and planktonic foraminifers (according to the current age model) (Fig. F2). The reasons for these discrepancies cannot at present be determined.

PALEOECOLOGICAL PARAMETERS

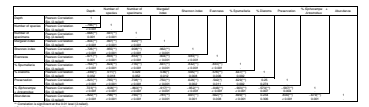
Preservation and Abundance

Although not a paleoecological parameter per se, careful examination of preservation is important to evaluate the bias in any paleoecological signal, and given that preservation is correlated to productivity, changes in preservation may provide important paleoceanographic information. Preservation can be analyzed based on fragmentation, dissolution, and recrystallization. Whereas recrystallization is not of major concern in the material (no chert was observed above Core 183-1138A-41R; 383 mbsf), fragmentation and dissolution of tests seriously affect the overall preservation of the faunas. As tectonic strain is virtually absent, the observed fragmentation can be used as a proxy of opal dissolution. The traditional classification of preservation into poor, moderate, and good applied to ODP micropaleontological samples thus may be translated into strongly dissolved/fragmented, moderately dissolved/fragmented, and weakly dissolved/fragmented faunas.

We tentatively classified preservation by visual estimation (Table T3) as done in most other ODP reports, but additionally we suggest that a more rigorous classification of dissolution can be applied. Only with a more quantitative measure of preservation can we hope to statistically test correlations between shell dissolution and productivity. As a first approximation, we calculated the percentage of *Siphocampe* and *Artostrobos* in our samples (Table T3). These genera are among the most robust taxa in our material and were observed in a fairly high absolute abundance throughout (Pl. P9, figs. 3–18; Pl. P10, figs. 1–8). Although the percentage of *Siphocampe* and *Artostrobos* may be controlled by additional factors and there are occasional other robust taxa in the samples, it is thought to be an independent quantitative proxy of fragmentation/dissolution. The higher the proportion of *Siphocampe* and *Artostrobos*, the higher dissolution is thought to be. Because *Siphocampe* is by far the more abundant of the two genera in our samples, we define the name “*Siphocampe* index” for the cumulative percentage of *Siphocampe* and *Artostrobos* in a sample. The significant correlation between the qualitative preservation evaluation and our *Siphocampe* index (Fig. F7) supports the suggestion that the latter may represent a proxy for radiolarian faunal preservation in the Oligocene. Both the qualitative preservation index and the *Siphocampe* proxy indicate a significant upward increase of preservation in the studied interval. The percentage of *Siphocampe* and *Artostrobos* declines from >80% in the lowest three samples to <10% in the upper part. The first well-preserved faunas are recorded in interval 183-1138A-35R-2, 105–107 cm, according to qualitative studies, whereas the *Siphocampe* index suggests that dissolution/fragmentation is reduced already in interval 183-1138A-35R-5, 20–22 cm.

Radiolarian abundance ranges from ~2,500 individuals per gram to >150,000 individuals per gram of dry sediment. Abundance increases upcore as significantly as preservation. Core 183-1138A-36R consistently yields abundances of <10,000 individuals per gram; abundance in Core 35R varies between ~12,000 and ~80,000 individuals per gram; and Core 34R always shows values >50,000 individuals per gram. Both

F7. Radiolarian faunal indices, Hole 1138A, p. 29.



the *Siphocampe* proxy and the qualitative estimate of preservation are significantly correlated with radiolarian abundance (Fig. F7). Following common arguments (Baldauf and Barron, 1990), both opal preservation and abundance of siliceous plankton groups are thought to co-vary with productivity, although the relationship is not simple (Nelson et al., 1995). Lazarus and Pallant (1989) have shown that Oligocene radiolarian abundance in the Labrador Sea is very well correlated to total organic carbon content and other independent proxy indicators of productivity. This, however, is not true for diatoms that are generally thought to be even better productivity proxies (Ragueneau et al., 2000).

Faunal Indices

All diversity indices are strongly correlated with each other and with our preservational proxies (Figs. F7, F8). This observation poses problems for the paleoecological interpretation of our data. All diversity indices and the abundance data are largely explained by fluctuations in preservation. Based on R^2 values, up to 90% of the variation in diversity can be explained by variations in preservation. Important exceptions are evenness and the percentage of diatoms, which are only weakly correlated with our qualitative measure of preservation but still exhibit very high correlations with our *Siphocampe* proxy. The weakest correlation in the whole data set is between the percentage of diatoms and radiolarian abundance. This may point to an independence of diatom and radiolarian abundance. If so, simple measurements of opal flux are probably not sufficient to characterize the productivity and interpret the signal, a point already emphasized by Diester-Haass (1995) and Ragueneau et al. (2000).

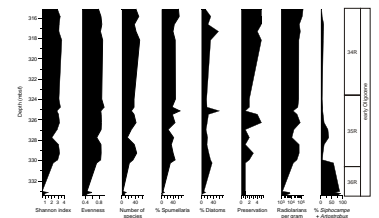
Even a principal component approach (Varimax rotation) does not help greatly to constrain primary patterns. Only one factor has an eigenvalue of >1 , explaining 77% of the total variance in the data set. Three factors explain 91% of the total variance. The first two factors are best interpreted as preservation. It is only the third factor that has the highest loadings on the percentage of diatoms in the assemblage, again indicating a somewhat decoupled pattern of diatom and radiolarian abundances.

When comparing only diversity patterns of equally well-preserved faunas in the section, no significant trend through the lower Oligocene is evident. The maximum diversity (Shannon and Margalef indices and species richness) is reached in Sample 183-1138A-34R-3, 105–107 cm, well below the top of the investigated time interval.

DISCUSSION

We test the hypothesis that changes in radiolarian faunal indices correspond to climatic change across the Eocene/Oligocene boundary interval and within the lower Oligocene, the null hypothesis being that radiolarian faunal indices develop independently from reconstructed changes in Earth-system parameters. In contrast to low latitudes, the sedimentary record of Eocene siliceous microplankton is generally patchy in southern high latitudes. This applies to diatoms as well as radiolarians (Baldauf, 1992; Baldauf and Barron, 1990). The observation that radiolarian preservation and accumulation rates increase gradually from the Eocene to the Oligocene has been made at many Southern Ocean Deep Sea Drilling Project and ODP sites (Table T4) including

F8. Oligocene-aged radiolarian faunas, Hole 1138A, p. 30.



T4. Mean preservation of radiolarian faunas, p. 38.

Antarctica. In nearly all regions where both Eocene and Oligocene sediments were studied, the Oligocene yields better-preserved faunas than the Eocene. This pattern is quite opposite to that in the tropics where the average preservation is much better in the late Eocene (Nigrini and Sanfilippo, 2000), but it is coherent with findings from northern high latitudes (Lazarus and Pallant, 1989). Although well-preserved faunas were recovered from the Eocene at several localities including the Kerguelen Plateau (Caulet, 1991), the mean preservation of radiolarians is significantly ($p < 0.001$, based on t-test) different between Eocene and Oligocene samples. One of the few exceptions is reported from the Falkland Plateau (Weaver, 1983), where well-preserved faunas are apparently present throughout the Eocene and Oligocene, although preservation varies between holes.

The general paucity of silica accumulation/preservation in many Eocene age southern high-latitude sites has been attributed to low productivity. Enhanced Oligocene silica accumulation and productivity are usually explained by high-latitude cooling, which increased latitudinal temperature gradients and led to stronger oceanic turnover and thus higher nutrient supply (Kennett, 1977). Tectonic uplift and enhanced weathering may also have contributed to increasing nutrient concentrations (Zachos et al., 1999). The development of the Antarctic Bottom Water formation may additionally have aided radiolarian preservation and declination of planktonic foraminiferal preservation (Diester-Haass, 1995). Although authors have often argued for a continuous and gradual climatic deterioration (Keller et al., 1992), it is now clear that cooling was punctuated in the earliest Oligocene, at least in the Southern Ocean (Wei, 1991; Zachos et al., 1999; Zachos et al., 2001).

Considering the arguments above, we are tempted to invoke climatic cooling and associated productivity fluctuations as the prime control of radiolarian preservation, abundance, and diversity. Although the relationship may not be as straightforward (Diester-Haass, 1996), the lower Oligocene opal maximum is usually associated with high values of other productivity proxies such as benthic foraminiferal accumulation rates and carbonate dissolution (Diester-Haass, 1996; Diester-Haass and Zahn, 1996). Carbonate dissolution is invoked as a paleoproductivity proxy owing to the increase of calcite dissolution with increasing organic carbon supply in a well-oxygenated environment (Diester-Haass, 1995). In our material, a temporal decoupling of the productivity proxies is evident. Carbonate dissolution appears to be most substantial in the upper Eocene and earliest Oligocene, judging from the incomplete stratigraphic record in Core 183-1138A-36R and the pronounced hiatus at the top of Core 183-1138A-37R (Fig. F2). Radiolarian preservation, in contrast, is not significantly enhanced before the uppermost lower Oligocene (Section 183-1138A-35R-2; Chron C10r or possibly Subchron C11n.1), immediately after the end of the condensed sequence of Core 183-1138A-36R. This pattern suggests regional differences on the Kerguelen Plateau. The sediments from Southern Kerguelen Plateau show a profound synchronous increase in productivity in the earliest Oligocene, Chron C13n (Sites 738 and 744; Diester-Haass, 1995, 1996; Zachos et al., 1999; Site 748; Wise et al., 1992), whereas the central and Northern Kerguelen Plateau (Sites 1138, 1139, and 1140) sediments record an increase in radiolarian and diatom preservation 3 to 4 m.y. later. This interpretation is consistent with the observation of Lazarus and Caulet (1993) that endemic radiolarian faunas, indicative of a distinct surface water mass, developed first during the late Eocene only close to the Antarctic continent on the Southern Kerguelen Plateau and

spread throughout the Antarctic region only later, during the Oligocene.

CONCLUSIONS

Radiolarians of late early Oligocene age from the Central Kerguelen Plateau exhibit an upsection tendency toward better preservation, higher abundance, and higher diversity. All these faunal characteristics are likely to be linked to cooling during the early Oligocene and a higher productivity of siliceous microplankton. In contrast to the Southern Kerguelen Plateau, the central and Northern Kerguelen Plateau exhibit a temporally decoupled pattern of different productivity proxies. Carbonate dissolution as identified by reduced carbonate accumulation rates and a pronounced hiatus occurred significantly earlier (late Eocene to early Oligocene; Chrons C17n to C11r) (Fig. F2) than the first record of well-preserved and abundant radiolarians (late early Oligocene; Chron C10r). We speculate that the productivity rise on the Central Kerguelen Plateau was first governed by nonsiliceous phytoplankton and was only later dominated by enhanced radiolarian and diatom abundance and preservation.

ACKNOWLEDGMENTS

This research used samples provided by the Ocean Drilling Program (ODP). ODP is sponsored by the U.S. National Science Foundation (NSF) and participating countries under management of Joint Oceanographic Institutions (JOI), Inc. Funding for this research was provided by the Deutsche Forschungsgemeinschaft (DFG) in the context of the graduate research program “Evolutionary Transformations and Mass Extinctions” and by DFG project Du 129/21.

We thank ODP for providing us with Leg 183 samples and the members of the Shipboard Scientific Party for sample collection. Thanks to Woody Wise, Helen Coxall, and James Arney for providing unpublished biostratigraphic data and to Maria Antretter for unpublished magnetic polarity data. Many thanks to the Shipboard Scientific Party for help and discussions, and to Jean-Pierre Caulet, Pat Quilty, Atsushi Takemura, and Paul Wallace for constructive reviews.

REFERENCES

- Abelmann, A., 1990. Oligocene to middle Miocene radiolarian stratigraphy of southern high latitudes from Leg 113, Sites 689–690, Maud Rise. *In* Barker, P.F., Kennett, J.P., et al., *Proc. ODP, Sci. Results*, 113: College Station, TX (Ocean Drilling Program), 675–708.
- Aubry, M.-P., 1992. Late Paleogene calcareous nannoplankton evolution: a tale of climatic deterioration. *In* Prothero, D.R., and Berggren, W.A. (Eds.), *Eocene-Oligocene Climatic and Biotic Evolution*: Princeton (Princeton Univ. Press), 272–309.
- Bailey, J.W., 1856. Notice of microscopic forms found in the soundings of the Sea of Kamtschatka—with a plate. *Am. J. Sci., Ser. 2*, 22:1–6.
- Baldauf, J.G., 1992. Middle Eocene through early Miocene diatom floral turnover. *In* Prothero, D.R., and Berggren, W.A. (Eds.), *Eocene-Oligocene Climatic and Biotic Evolution*: Princeton (Princeton Univ. Press), 310–326.
- Baldauf, J.G., and Barron, J.A., 1990. Evolution of biosiliceous sedimentation patterns—Eocene through Quaternary: paleoceanographic response to polar cooling. *In* Bleil, U., and Thiede, J. (Eds.), *Geological History of the Polar Oceans: Arctic Versus Antarctic*: Dordrecht (Kluwer Academic), 575–607.
- Bjørklund, K.R., 1976. Radiolaria from the Norwegian Sea, Leg 38 of the Deep Sea Drilling Project. *In* Talwani, M., Udintsev, G., et al., *Init. Repts. DSDP*, 38: Washington (U.S. Govt. Printing Office), 1101–1168.
- Blueford, J., 1988. Radiolarian biostratigraphy of siliceous Eocene deposits in central California. *Micropaleontology*, 34:236–258.
- Bütschli, O., 1882. Radiolaria. *In* Bronn, H.G. (Ed.), *Klassen und Ordnungen des Thier-Reichs, Wissenschaftlich dargestellt in Wort und Bild* (Col. 2): Leipzig (Wintersche Verlagshandlung), 332–478.
- Campbell, A.S., and Clark, B.L., 1944. Miocene radiolarian faunas from Southern California. *Spec. Pap.—Geol. Soc. Am.*, 51:1–76.
- Cande, S.C., and Kent, D.V., 1995. Revised calibration of the geomagnetic polarity timescale for the Late Cretaceous and Cenozoic. *J. Geophys. Res.*, 100:6093–6095.
- Carnevale, P., 1908. Radiolarie e silicoflagellati di Bergonzano (Reggio Emilia). *Veneto Sci. Lett. Arti Mem.*, 28:1–46.
- Caulet, J.P., 1986. Radiolarians from the southwest Pacific. *In* Kennett, J.P., von der Borch, C.C., et al., *Init. Repts. DSDP*, 90: Washington (U.S. Govt. Printing Office), 835–861.
- Caulet, J.-P., 1991. Radiolarians from the Kerguelen Plateau, Leg 119. *In* Barron, J., Larsen, B., et al., *Proc. ODP, Sci. Results*, 119: College Station, TX (Ocean Drilling Program), 513–546.
- Chen, P.-H., 1975. Antarctic radiolaria. *In* Hayes, D.E., Frakes, L.A., et al., *Init. Repts. DSDP*, 28: Washington (U.S. Govt. Printing Office), 437–513.
- Clark, B.L., and Campbell, A.S., 1942. Eocene radiolarian faunas from the Monte Diablo area, California. *Spec. Pap.—Geol. Soc. Am.*, 39:1–112.
- Crouch, E.M., and Hollis, C.J., 1996. Paleogene palynomorph and radiolarian biostratigraphy of DSDP Leg 29, Sites 280 and 281, South Tasman Rise. *Inst. Geol. Nucl. Sci., Sci. Rep.*, 96:19.
- Diester-Haass, L., 1995. Middle Eocene to early Oligocene paleoceanography of the Antarctic Ocean (Maud Rise, ODP Leg 13, Site 689): change from a low to a high productivity ocean. *Palaeogeogr., Palaeoclimatol., Palaeoecol.*, 113:311–334.
- , 1996. Late Eocene–Oligocene paleoceanography in the southern Indian Ocean (ODP Site 744). *Mar. Geol.*, 96:99–119.
- Diester-Haass, L., and Zahn, R., 1996. Eocene–Oligocene transition in the Southern Ocean: history of water mass circulation and biological productivity. *Geology*, 24:163–166.
- Dreyer, F., 1889. Morphologische Radiolarienstudien. 1. Die Pylombildungen in vergleichend-anatomischer und entwicklungsgeschichtlicher Beziehung bei Radiolar-

- ien und bei Protisten überhaupt, nebst System und Beschreibung neuer und der bis jetzt bekannten pylomatischen Spumellarien. *Jena. Z. Naturwiss.*, 23:1–138.
- Ehrenberg, C.G., 1844. Einige vorläufige Resultate seiner Untersuchungen der ihm von der Südpolreise des Capitain Ross, so wie von der Herren Schayer und Darwin zugekommenen Materialien über das Verhalten des kleinsten Lebens in den Oceanen und den grossten bisher zugänglichen Tiefen des Weltmeers vor. *Abh. K. Preuss. Akad. Wiss. Berlin*, 182–207.
- , 1847. Über die mikroskopischen kieselschaligen Polycystinen als mächtige Gebirgsmasse von Barbados und über das Verhältniss deraus mehr als 300 neuen Arten bestehenden ganz eigenthümlichen Formengruppe jener Felsmasse zu den jetzt lebenden Thieren und zur Kreidebildung. Eine neue Anregung zur Erforschung des Erdlebens. *K. Preuss. Akad. Wiss. Berlin, Bericht*, 1847:40–60.
- , 1854a. Weitere Ermittlungen über das Leben in grossen Tiefen des Oceans. *K. Preuss. Akad. Wiss. Berlin, Bericht*, 1854:305–328.
- , 1854b. *Mikrogeologie: Das Erden und Felsen schaffende Wirken des unsichtbar kleinen selbständigen Lebens auf der Erde*: Leipzig (Leopold Voss).
- , 1854c. Über das Organischen Leben des Meeresgrundes in bis 10,800 und 12,000 Fuss Tiefe. *K. Preuss. Akad. Wiss. Berlin, Bericht*, 1854:54–75.
- , 1858. Organischen Lebensformen in unerwartet grossen Tiefen des Mittelmeeres. *K. Preuss. Akad. Wiss. Berlin, Monatsberichte*, 1857:538–571.
- , 1861. Über die Tiefgrund-Verhältnisse des Oceans am Eingange der Davisstrasse und bei Island. *K. Preuss. Akad. Wiss. Berlin, Monatsberichte*, 1862:131–399.
- , 1872a. Mikrogeologische Studien als Zusammenfassung der Beobachtungen des kleinsten Lebens der Meeres-Tiefgrunde aller Zonen und dessen geologischen Einfluss. *K. Preuss. Akad. Wiss. Berlin, Monatsberichte*, 1872:265–322.
- , 1872b. Mikrogeologische Studien über das kleinste Leben der Meeres-Tiefgrunde aller Zonen und dessen geologischen Einfluss. *Abh. K. Akad. Wiss. Berlin*, 1872:131–399.
- , 1873. Grössere Felsproben des Polycystinen-Mergels von Barbados mit weiteren Erläuterungen. *K. Preuss. Akad. Wiss. Berlin, Monatsberichte*, 1873:213–263.
- , 1875. Fortsetzung der mikrogeologischen Studien als Gesamt-Uebersicht der mikroskopischen Paläontologie gleichartig analysirter Gebirgsarten der Erde, mit specieller Rücksicht auf den Polycystinen-Mergel von Barbados. *Abh. K. Akad. Wiss. Berlin*, 1875:1–225.
- Goll, R.M., 1968. Classification and phylogeny of Cenozoic Trissocyclidae (Radiolaria) in the Pacific and Caribbean basins, Part I. *J. Paleontol.*, 42:1409–1432.
- , 1978. Five Trissocyclid Radiolaria from Site 338. In Talwani, M., Udintsev, G., et al., *Init. Repts. DSDP*, 38, 39, 40, 41 (Suppl.): Washington (U.S. Govt. Printing Office), 177–191.
- Goll, R.M., and Bjørklund, K.R., 1989. A new radiolarian biostratigraphy for the Neogene of the Norwegian Sea: ODP Leg 104. In Eldholm, O., Thiede, J., Taylor, E., et al., *Proc. ODP, Sci. Results*, 104: College Station, TX (Ocean Drilling Program), 697–737.
- Haeckel, E., 1878. *Das Protistenreich. Eine populäre Übersicht über das Formengebiet der niedersten Lebewesen*, Kosmos. Zeitschrift für einheitliche Weltanschauung auf Grund der Entwicklungslehre. Leipzig (Ernst Gunther).
- , 1887. Report on the Radiolaria collected by H.M.S. *Challenger* during the years 1873–1876. *Rep. Sci. Results Voy. H.M.S. Challenger, 1873–1876, Zool.*, 18:1–1803.
- Hollis, C.J., Waghorn, D.B., Strong, C.P., and Crouch, E.M., 1997. *Integrated Paleogene Biostratigraphy of DSDP Site 277 (Leg 29): Foraminifera, Calcareous Nannofossils, Radiolaria, and Palynomorphs*: Lower Hutt (Inst. Geol. Nucl. Sci.).
- Jørgensen, E., 1905. The protist plankton and the diatoms in bottom samples. *Bergens Mus. Skr.*, 49–151.
- Keller, G., MacLeod, N., and Barrera, E., 1992. Eocene–Oligocene faunal turnover in planktic foraminifera, and Antarctic glaciation. In Prothero, D.R., and Berggren,

- W.A. (Eds.), *Eocene–Oligocene Climatic and Biotic Evolution*: Princeton (Princeton Univ. Press), 218–244.
- Kennett, J.P., 1977. Cenozoic evolution of Antarctic glaciation, the circum-Antarctic Ocean, and their impact on global paleoceanography. *J. Geophys. Res.*, 82:3843–3860.
- Lazarus, D., 1994. An improved cover-slip holder for preparing microslides of randomly distributed particles. *J. Sed. Res.*, A64:686.
- Lazarus, D., and Caulet, J.-P., 1993. Cenozoic Southern Ocean reconstructions from sedimentologic, radiolarian and other microfossil data. In Kennett, J.P., and Warnke, D.A. (Eds.), *The Antarctic Paleoenvironment: A Perspective on Global Change*. Antarct. Res. Ser., 60:145–174.
- Lazarus, D., and Pallant, A., 1989. Oligocene and Neogene radiolarians from the Labrador Sea, ODP Leg 105. In Srivastava, S.P., Arthur, M.A., Clement, B., et al., *Proc. ODP, Sci. Results*, 105: College Station, TX (Ocean Drilling Program), 349–380.
- Moore, T.C., 1973. Method of randomly distributing grains for microscopic examination. *J. Sed. Petrol.*, 43:904–906.
- Nelson, D.M., Treguer, P., Brzezinski, M.A., Leynaert, A., and Queguiner, B., 1995. Production and dissolution of biogenic silica in the ocean: revised global estimates, comparison with regional data and relationship to biogenic sedimentation. *Global Biogeochem. Cycles*, 9:359–372.
- Nigrini, C., 1977. Tropical Cenozoic Artostrobiidae (Radiolaria). *Micropaleontology*, 23, 241–269.
- Nigrini, C., and Lombardi, G., 1984. *A Guide to Miocene Radiolaria*. Spec. Publ.—Cushman Found. Foraminiferal Res., 22.
- Nigrini, C., and Sanfilippo, A., 2000. Paleogene radiolarians from Sites 998, 999, and 1001 in the Caribbean. In Leckie, R.M., Sigurdsson, H., Acton, G.D., and Draper, G. (Eds.), *Proc. ODP, Sci. Results*, 165, 57–81 [CD-ROM]. Available from: Ocean Drilling Program, Texas A&M University, College Station, TX 77845-9547, U.S.A.
- O'Connor, B.M., 1993. *Radiolaria from the Mahurangi Limestone*: Northland, New Zealand (Univ. of Auckland).
- , 1994. Seven new radiolarian species from the Oligocene of New Zealand. *Micropaleontology*, 40:337–350.
- , 1997. New Radiolaria from the Oligocene and early Miocene of Northland, New Zealand. *Micropaleontology*, 43:63–100.
- , 1999. Radiolaria from the late Eocene Oamaru diatomite, South Island, New Zealand. *Micropaleontology*, 45:1–55.
- , 2000. Stratigraphic and geographic distribution of Eocene–Miocene Radiolaria from the southwest Pacific. *Micropaleontology*, 46:189–228.
- Petrushevskaya, M.G., 1967. Radiolyarii otr'yadov Spumellaria i Nassellaria antarkticheskoi oblasti (Antarctic spumellariane and nassellariane radiolarians). In Andriyashev, A.P., and Ushakov, P.V. (Eds.), *Rez. Biol. Issled. Sov. Antarkt. Eksped. 1955–58*, 3:5–187.
- , 1971. Radiolyarii Nassellaria v planktone Mirovogo Okeana (Radiolarians of the Ocean). *Issled. Fauny Morei*, 9:1–294.
- , 1975. Cenozoic radiolarians of the Antarctic, Leg 29, DSDP. In Kennett, J.P., Houtz, R.E., et al., *Init. Repts. DSDP*, 29: Washington (U.S. Govt. Printing Office), 541–675.
- , 1979. Sequence of the radiolarian evolution in the Norwegian-Greenland Sea—evolution of the Norwegian Sea radiolarians from the Eocene to Recent. In Strelkov, A.A., and Petrushevskaya, M.G. (Eds.), *The History of the Microplankton of the Norwegian Sea (on the Deep Sea Drilling Materials)*. Explorations of the Fauna of the Sea, Acad. Sci. USSR, Zool. Inst., 23:77–85.
- Petrushevskaya, M.G., and Kozlova, G.E., 1972. Radiolaria, Leg 14, Deep Sea Drilling Project. In Hayes, D.E., Pimm, A.C., et al., *Init. Repts. DSDP*, 14: Washington (U.S. Govt. Printing Office), 495–648.

- Popofsky, A., 1912. Die Sphaerellarien des Warmwassergebietes. *Dtsch. Sudpolar-Exped., 1901–1903, Zool.*, 13:73–160.
- Ragueneau, O., Tréguer, P., Leynaert, A., Anderson, R.F., Brzezinski, M.A., DeMaster, D.J., Dugdale, R.C., Dymond, J., Fischer, G., Francois, R., Heinze, C., Maier-Reimer, E., Martin-Jézéquel, V., Nelson, D.M., and Quéguiner, B., 2000. A review of the Si cycle in the modern ocean: recent progress and missing gaps in the application of biogenic opal as a paleoproductivity proxy. *Global Planet. Change*, 26:317–365.
- Riedel, W.R., 1958. Radiolaria in Antarctic sediments. *Rep. B.A.N.Z. Antarct. Res. Exped., Ser. B*, 6:217–255.
- Riedel, W.R., and Sanfilippo, A., 1986. Radiolarian events and the Eocene–Oligocene boundary. In Pomerol, C., and Premoli Silva, I. (Eds.), *Terminal Eocene Events*: Amsterdam (Elsevier), 253–257.
- Sanfilippo, A., Burckle, L.H., Martini, E., and Riedel, W.R., 1973. Radiolarians, diatoms, silicoflagellates and calcareous nannofossils in the Mediterranean Neogene. *Micropaleontology*, 19:209–234.
- Sanfilippo, A., and Caulet, J.P., 1998. Taxonomy and evolution of Paleogene Antarctic and tropical Lophocyrtid radiolarians. *Micropaleontology*, 44:1–43.
- Sanfilippo, A., and Riedel, W.R., 1973. Cenozoic Radiolaria (exclusive of theoperids, artostrobiids and amphipyndacids) from the Gulf of Mexico, Deep Sea Drilling Project Leg 10. In Worzel, J.L., Bryant, W., et al., *Init. Repts. DSDP*, 10: Washington (U.S. Govt. Printing Office), 475–611.
- Sanfilippo, A., Riedel, W.R., Glass, B.P., and Kyte, F.T., 1985. Late Eocene microtektites and radiolarian extinctions on Barbados. *Nature*, 314:613–615.
- Shipboard Scientific Party, 2000. Site 1138. In Coffin, M.F., Frey, F.A., Wallace, P.J., et al., *Proc. ODP, Init. Repts.*, 183, 1–205 [Online]. Available from World Wide Web: <http://www-odp.tamu.edu/publications/183_IR/VOLUME/CHAPTERS/IR183_06.PDF>. [Cited 2000-04-20]
- Stöhr, E., 1880. Die Radiolarienfauna der Tripoli von Grotte, Provinz Girgenti in Sicilien (The radiolarian fauna of the Tripoli of Grotte, Girgenti Province, Sicily). *Paleontographica*, 26:69–124.
- Strong, C.P., Hollis, C.J., and Wilson, G.J., 1995. Foraminiferal, radiolarian, and dinoflagellate biostratigraphy of late Cretaceous to middle Eocene pelagic sediments (Muzzle Group), Mead Stream, Marlborough, New Zealand. *N. Z. J. Geol. Geophys.*, 38:171–209.
- Takemura, A., 1992. Radiolarian Paleogene biostratigraphy in the southern Indian Ocean, Leg 120. In Wise Jr., S.W., Schlich, R. et al. (Eds.), *Proc. ODP Sci. Results*, 120: College Station, TX (Ocean Drilling Program), 735–756.
- Takemura, A., and Ling, H.Y., 1997. Eocene and Oligocene radiolarian biostratigraphy from the Southern Ocean: correlation of ODP Legs 114 (Atlantic Ocean) and 120 (Indian Ocean). *Mar. Micropaleontol.*, 30:97–116.
- Vinassa de Regny, P.E., 1900. Radiolari Miocenici Italiani. *Mem. R. Acad. Sci. Inst. Bologna, Ser. 5*, 8:227–257.
- Weaver, F., Rögl, F., Haq, B.U., and Schrader, H.-J., 1976. Paleontological summary of Deep Sea Drilling results from Leg 35, Southwest Pacific Basin. In Hollister, C.D., Craddock, C., et al., *Init. Repts. DSDP*, 35: Washington (U.S. Govt. Printing Office), 531–537.
- Weaver, F.M., 1983. Cenozoic radiolarians from the southwest Atlantic, Falkland Plateau region, Deep Sea Drilling Project Leg 71. In Ludwig, W.J., Krasheninnikov, V.A., et al., *Init. Repts. DSDP*, 71 (Pt. 2): Washington (U.S. Govt. Printing Office), 667–686.
- Wei, W., 1991. Evidence for an earliest Oligocene abrupt cooling in the surface waters of the Southern Ocean. *Geology*, 19:780–783.
- Wise, S.W., Jr., Breza, J.R., Harwood, D.M., Wei, W., and Zachos, J.C., 1992. Paleogene glacial history of Antarctica in light of Leg 120 drilling results. In Wise, S.W., Jr., Schlich, R., et al., *Proc. ODP, Sci. Results*, 120: College Station, TX (Ocean Drilling Program), 1001–1028.

Zachos, J.C., Opdyke, B.N., Quinn, T.M., Jones, C.E., and Halliday, A.N., 1999. Early Cenozoic glaciation, antarctic weathering, and seawater $^{87}\text{Sr}/^{86}\text{Sr}$: is there a link? *Chem. Geol.*, 161:165–180.

Zachos, J.C., Pagani, M., Sloan, L., Thomas, E. and Billups, K., 2001. Trends, rhythms, and aberrations in global climate 65 Ma to present. *Science*, 292:686–693.

APPENDIX

Taxonomic List

- Actinomma holtedahli* Bjørklund gr. (Pl. P2, figs. 2–3); Bjørklund, 1976, p. 1121, pl. 20, figs. 8–9.
- Actinomma henningsmoeni* Goll and Bjørklund (Pl. P2, fig. 1); Goll and Bjørklund, 1989, p. 734, pl. 2, figs. 10–15.
- Amphistylus angelinus* (Clark and Campbell) (Pl. P1, fig. 3); Chen, 1975, p. 453, pl. 21, figs. 3–40.
- Amphistylus?* sp. A (Pl. P1, fig. 2).
- Amphistylus?* sp. Takemura, 1992, p. 741, pl. 5, fig. 9–10; Takemura and Ling, 1997, p. 108, pl. 1, fig. 3.
- Amphycraspedum proxilum?* Sanfilippo and Riedel (Pl. P4, fig. 9); Sanfilippo and Riedel, 1973, p. 608, pl. 10, figs. 7–11; pl. 11, figs. 1–5, pl. 28, figs. 3–5
- Amphymenium splendiararmatum* Clark and Campbell (Pl. P4, fig. 8); Clark and Campbell, 1942, p. 46, pl. 1, fig. 12; Sanfilippo and Riedel, 1973, p. 524, pl. 11, figs. 6–8; Petrushevskaya, 1975, p. 577, pl. 7, fig. 1; pl. 37, figs. 1–3; Caulet, 1991, p. 537; O'Connor, 1993, p. 40, pl. 2, figs. 16–17.
- Antarctissa longa* Petrushevskaya (Pl. P5, fig. 7); Petrushevskaya, 1975, p. 618, pl. 11, figs. 8–10.
- Antarctissa robusta* Petrushevskaya (Pl. P5, fig. 8); Petrushevskaya, 1975, p. 591, pl. 11, figs. 21–22.
- Antarctissa* sp. cf. *A. conradae* Chen (Pl. P5, figs. 9–10); cf. Chen, 1975, p. 457, pl. 17, figs. 1–5.
- Remarks:** Both specimens look like the species described by Chen, but poor preservation prevents a definite assignment.
- Artostrobos annulatus* (Bailey) gr. (Pl. P9, figs. 3–4).
- Cornutella annulatus* Bailey, 1856, p. 3, fig. 5; Petrushevskaya, 1975, p. 579, pl. 10, figs. 4–5.
- Artostrobos stathmeporoides* (Petrushevskaya) nov. comb. (Pl. P10, figs. 1–2); *Lithomitrella stathmeporoides* Petrushevskaya, 1979, p. 151, fig. 411, not fig. 410.
- Remarks:** Comparison with the type material of Ehrenberg showed that the species has no resemblance with *Eucyrtidium acephala*, the type species of *Lithomitrella*, but has to be assigned to *Artostrobos*. Petrushevskaya described this species as lacking a cephalic horn. Its depicted holotype, however, bears a horn, just like specimens.
- Artostrobos pusillum* (Ehrenberg) gr. (Pl. P9, figs. 6–10); *Eucyrtidium pusillum* Ehrenberg, 1873, p. 232, pl. 11, fig. 6; not Petrushevskaya, 1971, pl. 92, fig. 5, not *A. pusillum* (Ehrenberg), Petrushevskaya, 1975, p. 578, pl. 26, figs. 1–2.
- Remarks:** The holotype of *A. pusillum* in the Ehrenberg collection (*E. pusillum*) shows no similarity with *A. pusillum* described by Petrushevskaya, 1975.
- Artostrobos pretabulatus* Petrushevskaya (Pl. P9, fig. 5); Takemura, 1992, p. 745, pl. 5, fig. 12; Crouch and Hollis, 1996, p. 26.

Axoprunum bispiculum (Popofsky) (Pl. P1, fig. 13)

- Stylocontarium bispiculum* Popofsky, 1912, p. 91, pl. 2, fig. 2; Chen, 1975, p. 454, pl. 21, figs. 1–2.
- Axoprunum bispiculum* (Popofsky) Takemura, 1992, p. 741, pl. 1, figs. 1–2; Hollis et al., 1997, p. 43, pl. 1, fig. 14.

Axoprunum irregularis Takemura (Pl. **P1**, figs. 15–16); Takemura, 1992, p. 752, pl. 3, figs. 8–11.

***Axoprunum pierinae* (Clark and Campbell)**
(Pl. **P1**, fig. 14)

Lithatractus pierinae Clark and Campbell, 1942, p. 34, pl. 5, fig. 25.

Axoprunum pieridae (Clark and Campbell), gr., Sanfilippo and Riedel, 1973, p. 488, pl. 1, figs. 6–11; pl. 23, fig. 3; Petrushevskaya, 1975, p. 571; Caulet, 1991, p. 537; Takemura, 1992, p. 742, pl. 6, figs. 3–6; Strong et al., 1995, p. 208, fig. 10c; Crouch and Hollis, 1996, p. 26; Takemura, 1997, p. 112, pl. 1, fig. 1; O'Connor, 1999, pl. 10, fig. 12.

Botryocella pauciperforata O'Connor (Pl. **P6**, fig. 11); O'Connor, 1999, p. 42, pl. 5, figs. 20a–24.

Botryostrobus kerguelensis Caulet (Pl. **P9**, fig. 2); Caulet, 1991, p. 535, pl. 3, figs. 6–8.

Ceratocyrtis mashae Bjørklund (Pl. **P6**, fig. 5); Bjørklund, 1976, p. 1125, pl. 17, figs. 1–8.

Ceratocyrtis robustus? Bjørklund (Pl. **P6**, figs. 3–4); Bjørklund, 1976, p. 1125, pl. 17, figs. 9–10.

Remarks: Our specimens are very similar to Bjørklund's species, but poor preservation prevents a definite statement.

Ceratocyrtis sp. aff. *C. stigi* (Bjørklund), nov. comb (Pl. **P6**, fig. 2); aff. *Lithomelissa stigi* Bjørklund, 1976, p. 1125, pl. 15, figs. 12–17.

***Ceratocyrtis stigi* (Bjørklund), nov. comb**
(Pl. **P6**, fig. 1)

Lithomelissa stigi Bjørklund, 1976, p. 1125, pl. 15, figs. 12–17.

Ceratocyrtis panicula Petrushevskaya, Petrushevskaya and Kozlova, 1972, p. 115.

Lithomelissa sp. C Chen, 1975, p. 458, pl. 11, figs. 4–5.

Lithomelissa sp. Bjørklund, 1976, pl. 15, figs. 9–11.

Ceratocyrtis stigi (Bjørklund), Nigrini and Lombardi, 1984, p. N13, pl. 15, fig. 7.

***Cornutella profunda* Ehrenberg gr.**
(Pl. **P6**, figs. 13–15)

Cornutella clathrata s.s. *profunda* Ehrenberg, 1854b, pl. 35BIV, fig. 24.

Cornutella verrucosa Ehrenberg, 1872a, p. 287; Ehrenberg, 1872b, pl. 9, fig. 16.

Cornutella profunda Ehrenberg, 1858, p. 31; Riedel, 1958, p. 232, pl. 3, figs. 1–2; Petrushevskaya, 1975, p. 587, pl. 13, figs. 32–33.

Corythospyris fiscella Goll gr. (Pl. **P8**, figs. 1–4); Goll, 1978, p. 178, pl. 5, figs. 1–21; Abelman, 1990, p. 695, pl. 4, figs. 4a, 4b, 7.

Corythospyris jubata Goll (Pl. **P8**, fig. 5); Goll, 1978, p. 177, pl. 4, figs. 1, 2, 4, 5, 7–17.

Cyrtolagena laguncula Haeckel (Pl. **P7**, fig. 14); Haeckel, 1878, p. 1451, pl. 75, fig. 10; Petrushevskaya, 1975, p. 583, pl. 14, figs. 3–4.

- Dendrospyris stabilis* Goll (Pl. **P8**, figs. 7–8); Goll, 1968, p. 1422–1423, pl. 173, figs. 16–18.
- Dictyophimus archipilium* Petrushevskaya (Pl. **P7**, fig. 10); Petrushevskaya, 1975, p. 583, pl. 25, figs. 1–2.
- Dictyophimus craticula* Ehrenberg (Pl. **P7**, fig. 9); Sanfilippo and Riedel, 1973, p. 609, pl. 19, fig. 1; pl. 33, fig. 11.
- Dictyophimus* sp. aff. *D. archipilium* Petrushevskaya (Pl. **P7**, fig. 11); aff. Petrushevskaya, 1975, p. 583, pl. 25, figs. 1–2.
- Dictyoprora physothorax* Caulet (Pl. **P10**, figs. 9–10); Caulet, 1991, p. 535, pl. 3, fig. 11.
- Dryomyomma? elegans* Jørgensen gr. (Pl. **P2**, figs. 4–5); Bjørklund, 1976, p. 1132, pl. 3, figs. 1–4.
- Eucyrtidium spinosum* Takemura (Pl. **P7**, fig. 5); Takemura, 1992, p. 746, pl. 5, figs. 5–8.

***Eucyrtidium punctatum* (Ehrenberg)**
(Pl. **P7**, fig. 6)

- Lithocampe punctata* Ehrenberg, 1844, p. 84.
- Eucyrtidium punctatum* (Ehrenberg), Ehrenberg, 1847, p. 43; Ehrenberg, 1854c, pl. 22, fig. 24.
- Artostrobos zitteli* Vinassa de Regny, 1900, p. 586, pl. 3, fig. 19.
- Eucyrtidium punctatum* (Ehrenberg) group, Chen, 1975, p. 495, pl. 15, fig. 8; Sanfilippo et al., 1973, p. 221, pl. 5, figs. 15–16.
- Eucyrtidium punctatum* (Ehrenberg) group, Weaver et al., 1976, p. 581, pl. 4, figs. 1–2; pl. 8, figs. 4–6.
- Eucyrtidium punctatum* Caulet, 1986, p. 852, pl. 5, fig. 9.

***Eurystomoskevos petrushevskae* Caulet**
(Pl. **P7**, fig. 13)

- Diplocyclas* sp. A Petrushevskaya and Kozlova, 1972, p. 541, pl. 33, figs. 14–16; Petrushevskaya, 1975, p. 587, pl. 24, fig. 4.
- Eurystomoskevos petrushevskae* Caulet, 1991, p. 536, pl. 3, figs. 14–15.
- Lithomelissa gelasinus* O'Connor (Pl. **P5**, fig. 4); O'Connor, 1997, p. 69, pl. 2, figs. 3–6; pl. 6, figs. 6–9, text-fig. 4; Hollis et al., 1997, p. 52, pl. 3, figs. 15–16; O'Connor, 2000, p. 206, pl. 1, figs. 7a, 7b, 8a, 8b, 9a, 9b.
- Lithomelissa* sp. aff. *Lithomelissa ehrenbergi* Bütschli (Pl. **P5**, fig. 5); aff. Bütschli, 1882, p. 519, fig. 21.
- Lithomelissa dupliphysa* Caulet (Pl. **P5**, fig. 1); Caulet, 1991, p. 534, pl. 2, fig. 4.
- Lithomelissa tricornis* Chen (Pl. **P5**, fig. 3); Chen, 1975, p. 458, pl. 8, figs. 6–7; Abelmann, 1990, p. 695, pl. 5, fig. 3; Takemura, 1992, p. 744, pl. 2, figs. 11–12; Hollis et al., 1997, p. 53.
- Lophocytis (Apoplanius) klydus?* Sanfilippo and Caulet (Pl. **P7**, fig. 8); Sanfilippo and Caulet, 1998, p. 12, pl. 3a, figs. 11–12; pl. 3b, figs. 10–11; pl. 5, figs. 4a, 4b, 5a, 5b, 8, 10, 11.
- Lophophaena capito* Ehrenberg (Pl. **P6**, fig. 6); Ehrenberg, 1873, p. 242; 1875, pl. 8, fig. 6; Crouch and Hollis, 1996, p. 26.

Lychnocanoma conica (Clark and Campbell)

(Pl. P7, fig. 1)

Lychnocanoma conicum Clark and Campbell, 1942, p. 71, pl. 9, fig. 38.

Lychnocanella conica Petrushevskaya, 1975, p. 583, pl. 12, figs. 2, 11–15.

Lychnocanoma conica Abelmann, 1990, p. 697, pl. 6, fig. 8; pl. 7, fig. 1a, 1b.

Lychnocanoma sp. cf. *Lychnocanoma babylonis* (Clark and Campbell) (Pl. P7, fig. 2); cf. *Dictyophimus babylonis* Clark and Campbell, 1942, p. 67, pl. 9, figs. 32, 36.

Lychnocanoma babylonis (Clark and Campbell).

Lychnocanoma tripodium (Ehrenberg)

(Pl. P7, fig. 3)

Lychnocanium tripodium Ehrenberg, 1875, pl. 7, fig. 2.

Lychnocanoma tripodium (Ehrenberg), in Haeckel, 1887, p. 1229.

Perichlamydidium limbatum Ehrenberg (Pl. P4, fig. 3); Ehrenberg, 1854b, pl. 22, fig. 20; Haeckel, 1887, p. 514; Petrushevskaya, 1975, p. 575, pl. 6, fig. 11; pl. 39, figs. 1–4.

Plannapus hornibrooki O'Connor (Pl. P10, fig. 12); O'Connor, 1999, p. 7, pl. 1, figs. 7a–10; pl. 5, figs. 8a–11, text-fig. 2; O'Connor, 2000, p. 207, pl. 1, figs. 10a, 10b–11a, 11b.

Plannapus mauricei O'Connor (Pl. P10, fig. 13); O'Connor, 1999, p. 8, pl. 1, figs. 11–14; pl. 5, figs. 12a–15; O'Connor, 2000, p. 208, pl. 1, figs. 12a, 12b–13a, 13b.

Genus *PRUNOPYLE* Stöhr

Remarks: Spumellarians with pylomes, a well-developed cortical shell, and internal spiral or spongy structures (“prunoids”) were first clearly described by Stöhr (1880) from Sicily. His drawings, however, do not clearly match any known material from more recent studies either of the Mediterranean region or the Antarctic. Stöhr also did not leave behind any type material for reanalysis. Thus, his genus concepts cannot be used with any degree of confidence. Dreyer (1889) described several prunoid species and genera, working with the same set of *Challenger* expedition materials used by Haeckel. As these materials are still available for restudy, it seems best to use this publication for determining the priority of generic concepts. Dreyer’s family level concepts were the artificial ones introduced by Haeckel, and partly in consequence, he included many distantly related forms in his analysis. He also considered that any larger than average cortical shell pore was the same homologous structure—a pylome. Thus, his new genera often would now be assigned to widely different families. Dreyer’s type species for the genus *Prunopyle* appears, on examination of the illustration and text description, to actually be a stylosphaerid, thus not suitable for prunoid taxa, as defined here. Although the distinction between Dreyer’s genera that do refer to prunoid morphologies is not yet fully clear, the closest match to our material is his genus *Larcopyle*, and we tentatively assign our material to it.

Prunopyle? fragilis (Stöhr)

(Pl. P3, fig. 13)

Ommatodiscus fragilis Stöhr, 1880, p. 116, pl. 6, fig. 10.

Lithocarpium fragilis (Stöhr), Petrushevskaya, 1975, p. 572, pl. 4, figs. 2–4.

Prunopyle frakesi Chen, 1975, p. 454, pl. 10, figs. 1–3.

Prunopyle sp. B gr. Abelman, 1990, p. 693, pl. 4, fig. 3a, 3b.

Prunopyle fragilis (Stöhr), Crouch and Hollis, 1996, p. 26; Hollis et al., 1997, p. 47, pl. 2, figs. 28–29; O'Connor, 1999, pl. 8, fig. 8.

Prunopyle? hayesi Chen (Pl. **P3**, fig. 9); Chen, 1975, p. 454, pl. 9, figs. 4–5.

***Prunopyle? polyacantha* Clark and Campbell gr.**

(Pl. **P3**, figs. 11, 12)

Larnacantha polyacantha Campbell and Clark, 1944 p. 30, pl. 5, fig. 4; Caulet, 1991, p. 539; Crouch and Hollis, 1996, p. 26.

Lithocarpium polyacantha (Campbell and Clark), Petrushevskaya, 1975 (in part), p. 572, pl. 3, figs. 6–8, fig. 9 (not pl. 29, fig. 6); Abelman, 1990, p. 694, pl. 4, fig. 2; O'Connor, 1993, p. 37, pl. 2, figs. 12–13.

Prunopyle? titan Clark and Campbell (Pl. **P3**, fig. 14); *Prunopyle titan* Campbell and Clark, 1944a, p. 20, pl. 3, figs. 1–3; Caulet, 1986, p. 853; Abelman, 1990, p. 693, fig. 16.

Prunopyle cf. *titan* Clark and Campbell; O'Connor, 1993, p. 33, pl. 1, figs. 16–17, pl. 10, fig. 1; Crouch and Hollis, 1996, p. 26; Hollis et al., 1997, p. 49, pl. 2, figs. 31–32; O'Connor, 1999, pl. 1, fig. 9.

Prunopyle? tryppyrena Caulet (Pl. **P3**, fig. 10); Caulet, 1991, p. 533, pl. 1, figs. 5–7.

***Pseudodictyophimus gracilipes* (Bailey) gr.**

(Pl. **P7**, fig. 12)

Dictyophimus gracilipes Bailey, 1856, p. 4, pl. 1, fig. 8.

Pseudodictyophimus gracilipes (Bailey), Petrushevskaya, 1971, p. 93, figs. 47–49; 1975, p. 592, pl. 11, fig. 17; Caulet, 1986, p. 853.

Pterosyringium hamata O'Connor (Pl. **P5**, fig. 2); O'Connor, 1999, p. 27, pl. 4, figs. 16–21b; pl. 7, figs. 20a–23.

***Siphocampe acephala* (Ehrenberg) gr.**

(Pl. **P9**, figs. 14–17)

Eucyrtidium elegans Ehrenberg, 1854b, pl. 36, fig. 17; 1875, pl. 11, fig. 12.

Siphocampe acephala (Ehrenberg) gr., Hollis et al., 1997, p. 54, pl. 4, figs. 8–20.

Siphocampe cf. *acephala* (Ehrenberg), Nigrini, 1977, p. 254, pl. 3, fig. 5.

Siphocampe missilis O'Connor, 1994, p. 340, pl. 1, figs. 7, 9, 12; pl. 3, figs. 8–12; O'Connor, 1999, p. 36, pl. 9, fig. 41.

***Siphocampe arachnea* (Ehrenberg) gr.**

(Pl. **P9**, figs. 12–13)

Eucyrtidium lineatum arachneum Ehrenberg, 1861, p. 229.

Lithomitra arachnea (Ehrenberg), Riedel, 1958, p. 242, pl. 4, figs. 7–8.

Siphocampe arachnea (Ehrenberg) gr., Nigrini, 1977, p. 255; Caulet, 1991, p. 539.

***Siphocampe nodosaria* (Haeckel)**

(Pl. **P9**, fig. 11)

Lithomitra nodosaria Haeckel, 1887, p. 1484, pl. 9, fig. 1.

Siphocampe arachnea Abelmann, 1990, p. 698, pl. 8, fig. 4a, 4b.

Siphocampe imbricata Caulet, 1991, p. 539, pl. 3, fig. 13.

Siphocampe nodosaria Hollis et al., 1997, p. 55, pl. 4, figs. 28–32.

Siphocampe? elizabethae sensu Hollis (Pl. **P9**, fig. 18); Hollis et al., 1997, p. 55, pl. 4, fig. 27.

Spirocyrtis greeni O'Connor (Pl. **P9**, fig. 1); O'Connor, 1999, p. 8, pl. 1, figs. 15–20b; pl. 5, figs. 16a–19.

Spongodiscus sp. aff. *Spongodiscus maculatus* Clark and Campbell (Pl. **P4**, fig. 1); aff. Clark and Campbell, 1942, emend. Blueford, 1988, p. 254, pl. 7, figs. 6–7.

Spongopyle osculosa Dreyer (Pl. **P4**, fig. 2); Dreyer, 1889, p. 42, pl. 11, figs. 99–100; Abelmann, 1990, p. 693, pl. 3, fig. 11.

Stylodictya aculeata Jørgensen (Pl. **P4**, fig. 6); Jørgensen, 1905, p. 119, pl. 10, fig. 41; Petrushevskaya, 1967, p. 35, pl. 17, figs. 1–3; Abelmann, 1990, p. 693, pl. 3, fig. 9.

Stylodictya ocellata? Ehrenberg (Pl. **P4**, fig. 5); Ehrenberg, 1873, p. 258; Ehrenberg, 1875, pl. 23, fig. 7.

Stylodictya validispina Jørgensen (Pl. **P4**, fig. 7); Jørgensen, 1905, p. 119, pl. 10, fig. 40; Petrushevskaya, 1967, p. 33, fig. 17, IV–V; Abelmann, 1990, p. 693, pl. 3, fig. 10.

***Stylosphaera radiosa* Ehrenberg gr.**

(Pl. **P1**, figs. 6–8)

Stylosphaera radiosa Ehrenberg, 1854a, p. 256; Ehrenberg, 1875, pl. 24, fig. 5.

Druppatractus? agostinelli Carnevale, 1908, p. 20, pl. 3, fig. 10.

Amphisphaera radiosa (Ehrenberg) group Petrushevskaya, 1975, p. 570, pl. 2, figs. 18–20.

Stylosphaera coronata coronata Ehrenberg, Chen, 1975, p. 455, pl. 5, figs. 1–2.

***Tripodiscinus clavipes* (Clark and Campbell)**

(Pl. **P6**, fig. 9)

Tripilidium clavipes Clark and Campbell, 1942, p. 64, pl. 9, fig. 29.

Tripodiscinus clavipes Hollis et al., 1997, p. 53, pl. 3, figs. 28–29.

Figure F1. Location of the Kerguelen Plateau with Leg 183 sites and other sites discussed in the text. Underlined numbers indicate Leg 183 sites that have been examined for radiolarians. This study describes Oligocene-aged radiolarians from Site 1138.

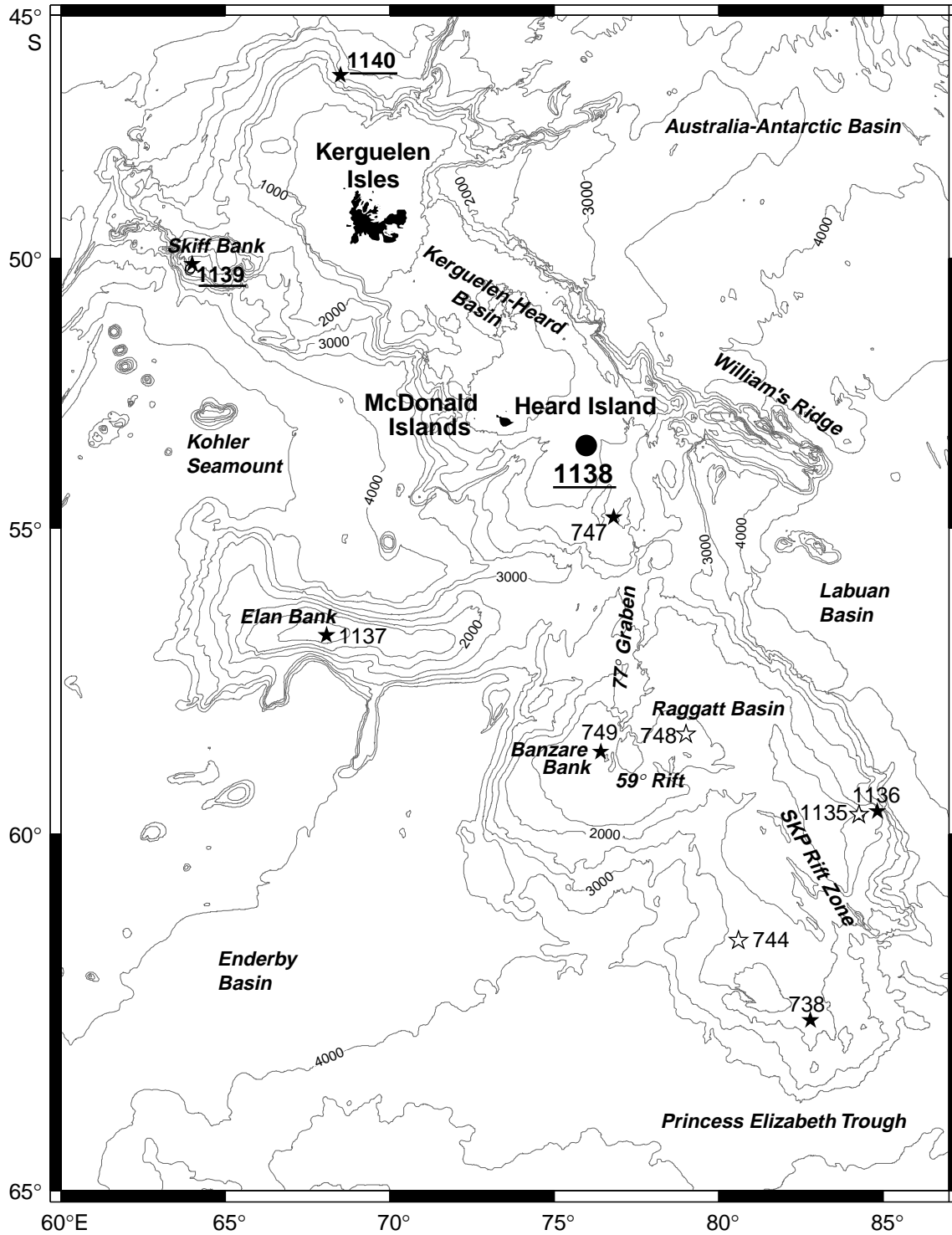


Figure F2. Age-depth plot for the Eocene–Oligocene interval of Hole 1138A. The curve is based on biostratigraphic and magnetostratigraphic data (M. Antretter et al., unpubl. data). The magnetostratigraphic timescale is taken from Cande and Kent (1995). Normal polarity is shown in black; reversed polarity is shown in gray. The black line is the estimated age-depth curve; the uncertainty interval is shaded yellow. All magnetostratigraphic chrons that can be assigned to a specific polarity interval of a core are plotted as boxes at the same depth as the core interval. The age curve must run through one of these boxes. Biostratigraphic events and zones used to constrain the magnetostratigraphic assignments are as follows: Nannofossils: N20: FO *Discoaster multiradiatus* (457.30–458.45 mbsf; 56.2 Ma); N21: LO *Fasciculithus tympaniformis* (449.60–450.35 mbsf; 5.3 Ma); N22: FO *Tribrachiatus orthostylus* (449.60–450.35 mbsf; 53.6 Ma); N23: FO *Discoaster lodoensis* (441.92–448.85 mbsf; 52.8 Ma); N24: FO *Discoaster subloensis* (441.92–448.85 mbsf; 49.7 Ma); N25: FO *Nannotetrina* spp. (429.55–430.38 mbsf; 47.3 Ma); N26: FO *Chiasmolithus gigas* (422.08–429.55 mbsf; 46.1 Ma); N27: LO *C. gigas* (405.90–406.65 mbsf; 44.5 Ma); N28: FO *Reticulofenestra bisecta* (356.20–357.19 mbsf; 38.0 Ma); N29: LO *Chiasmolithus solitus* (351.10–351.94 mbsf; 37.9 Ma); N30: FO *Chiasmolithus* (346.60–347.35 mbsf; 37.1 Ma); N31: FO *Chiasmolithus oamaruensis* (345.85–346.60 mbsf; 37.0 Ma); N32: FO *Isthmolithus recurvus* (344.35–345.10 mbsf; 35.7–36.3 Ma); N33: FO *Reticulofenestra oamaruensis* (342.85–343.60 mbsf; 35.4 Ma); N34–N39: *Chiasmolithus altus* zone (278.21–330.78 mbsf; 26.0–31.3 Ma); N40: *R. bisecta* zone (269.41 mbsf; 23.8–26.1 Ma); and N41: Zone CN2–CN1 (261.81 mbsf; 18.3–23.9 Ma). Foraminifers: F17–F19, F21: Zone AP11–AP10 (357.2–383.3 mbsf; 37.7–42.9 Ma); F20: LO *Acarinina bullbrooki* (354.5–365.6 mbsf; 40.5 Ma); F22: LO *Acarinina primitiva* (349.35–350.85 mbsf; 39.0 Ma); F23: LO *Acarinina collactea* (339.8–343.4 mbsf; 37.7 Ma); F24: LO *Subbotina linaperta* (339.8–343.4 mbsf; 37.7 Ma); F25: LO *Globigerinatheka index* (339.8–343.4 mbsf; 34.3 Ma); F26: Zone AP13 (340.60 mbsf; 30.0–34.3 Ma); F27: LO *Subbotina angiporoides* (324.45–335.25 mbsf; 30.0–30.5 Ma); F28–F29: Zone AP16–AP15 (278.21–285.85 mbsf; 23.8–28.5 Ma); F30: LO *Globigerina euapertura* (261.81–269.41 mbsf; 23.8 Ma); and F31: Zone NK1 (261.81 mbsf; 21.6–23.8 Ma). (Figure shown on next page.)

Figure F2 (continued). (Caption shown on previous page.)

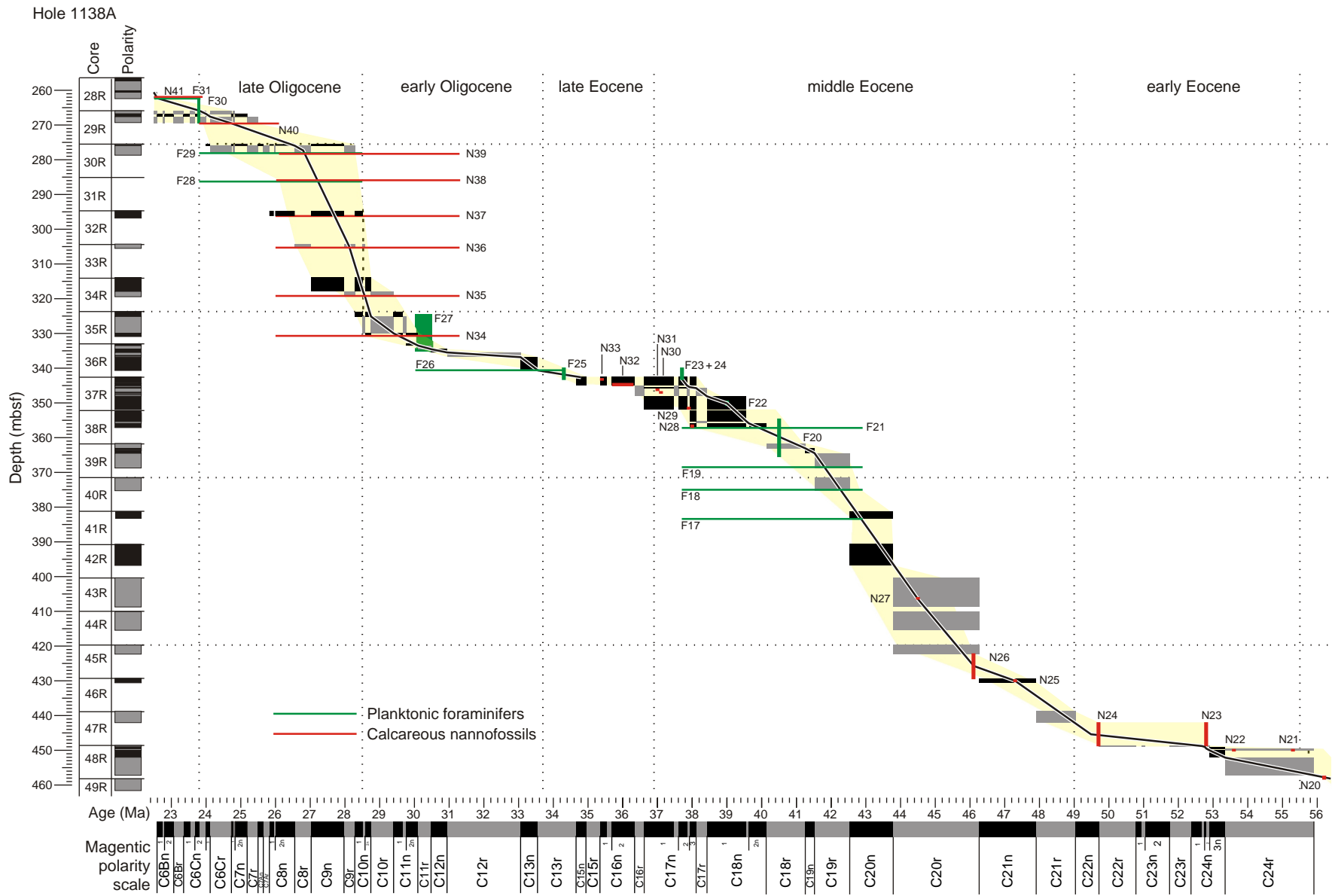


Figure F6. Oligocene radiolarian stratigraphic marker taxa in Hole 1138A. The ranges of the marker taxa of Takemura and Ling (1997) are indicated. There is a discrepancy between the published radiolarian zonation and our radiolarian ages. See Figure F2, p. 23, for magnetostratigraphic interpretation. Dashed line indicates species would be expected but was not found.

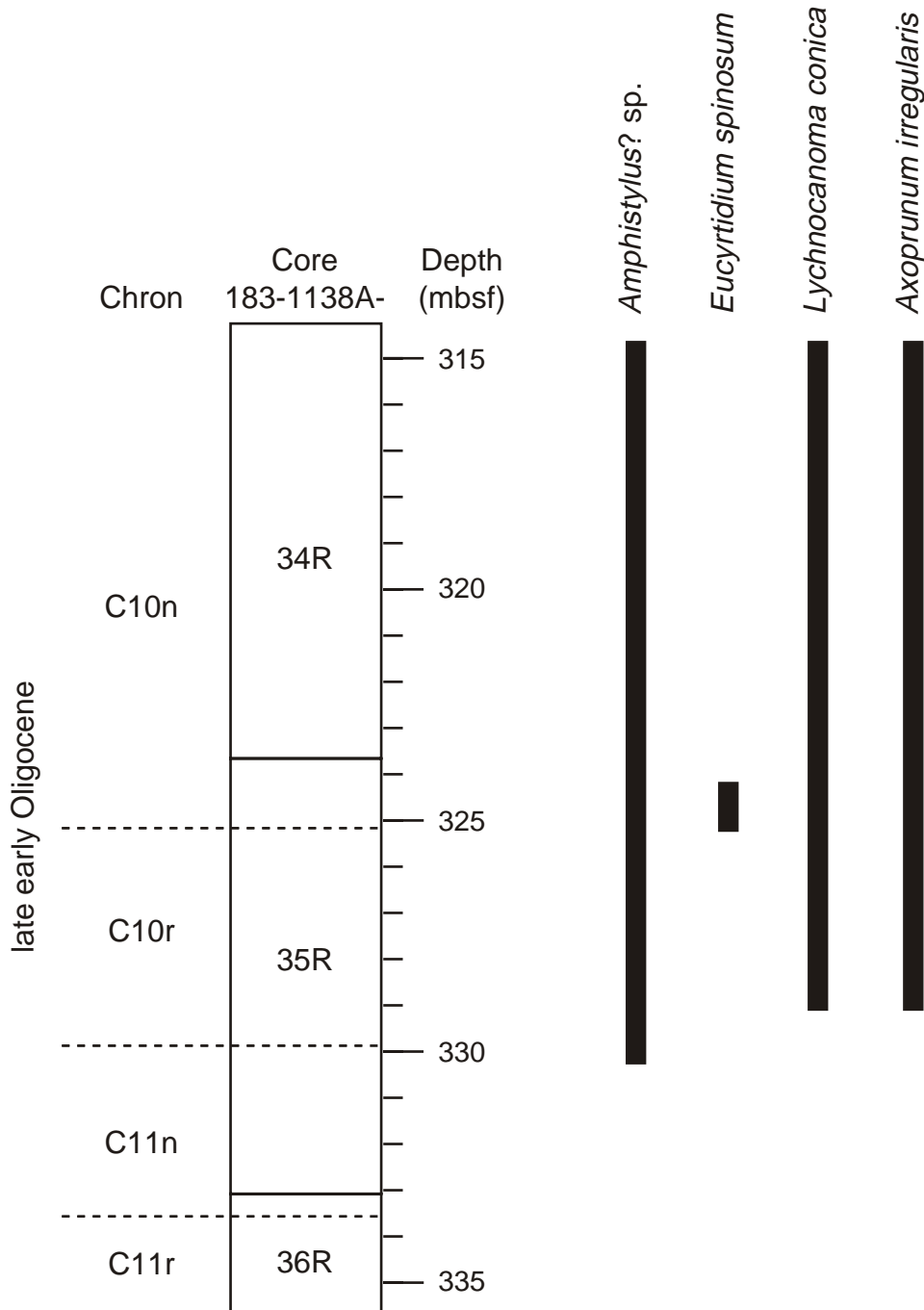


Figure F7. Correlations between radiolarian faunal indices in Hole 1138A, Cores 183-1138A-36R through 34R (early Oligocene).

		Depth	Number of species	Number of specimens	Margalef index	Shannon index	Evenness	% Spumellaria	% Diatoms	Preservation	% <i>Siphocampe</i> + <i>Artostrobos</i>	Abundance
Depth	Pearson Correlation	1										
	Sig. (2-tailed)	.										
Number of species	Pearson Correlation	-.796(**)	1									
	Sig. (2-tailed)	< 0.001	.									
Number of specimens	Pearson Correlation	-.668(**)	.941(**)	1								
	Sig. (2-tailed)	0.001	< 0.001	.								
Margalef index	Pearson Correlation	-.804(**)	.997(**)	.920(**)	1							
	Sig. (2-tailed)	< 0.001	< 0.001	< 0.001	.							
Shannon index	Pearson Correlation	-.726(**)	.955(**)	.908(**)	.962(**)	1						
	Sig. (2-tailed)	< 0.001	< 0.001	< 0.001	< 0.001	.						
Evenness	Pearson Correlation	-.671(**)	.893(**)	.853(**)	.904(**)	.983(**)	1					
	Sig. (2-tailed)	0.001	< 0.001	< 0.001	< 0.001	< 0.001	.					
% Spumellaria	Pearson Correlation	-.764(**)	.824(**)	.735(**)	.841(**)	.842(**)	.833(**)	1				
	Sig. (2-tailed)	< 0.001	< 0.001	< 0.001	< 0.001	< 0.001	< 0.001	.				
% Diatoms	Pearson Correlation	-.469(*)	.511(*)	0.429	.536(*)	.565(**)	.578(**)	.647(**)	1			
	Sig. (2-tailed)	0.032	0.018	0.052	0.012	0.008	0.006	0.002	.			
Preservation	Pearson Correlation	-.823(**)	.765(**)	.708(**)	.750(**)	.628(**)	.542(*)	.629(**)	0.25	1		
	Sig. (2-tailed)	< 0.001	< 0.001	< 0.001	< 0.001	0.002	0.011	0.002	0.274	.		
% <i>Siphocampe</i> + <i>Artostrobos</i>	Pearson Correlation	.723(**)	-.908(**)	-.860(**)	-.917(**)	-.952(**)	-.946(**)	-.903(**)	-.570(**)	-.597(**)	1	
	Sig. (2-tailed)	< 0.001	< 0.001	< 0.001	< 0.001	< 0.001	< 0.001	< 0.001	0.007	0.004	.	
Abundance	Pearson Correlation	-.822(**)	.796(**)	.765(**)	.781(**)	.661(**)	.562(**)	.699(**)	0.234	.800(**)	-.679(**)	1
	Sig. (2-tailed)	< 0.001	< 0.001	< 0.001	< 0.001	0.001	0.008	< 0.001	0.306	< 0.001	0.001	.

** Correlation is significant at the 0.01 level (2-tailed).

* Correlation is significant at the 0.05 level (2-tailed).

Figure F8. Quantitative characterization of Oligocene-aged radiolarian faunas in Hole 1138A. The Shannon diversity index, evenness, number of species, percentage of spumellarians, percentage of diatoms, preservation, and radiolarian abundance per gram of dry sediment are indicated. In addition, a newly proposed proxy for radiolarian preservation (% *Siphocampe* + *Artostrobos* = *Siphocampe* proxy) is indicated. Note the distinct trends of all parameters and strongly fluctuating diversity, abundance, and preservation in the lower part of section.

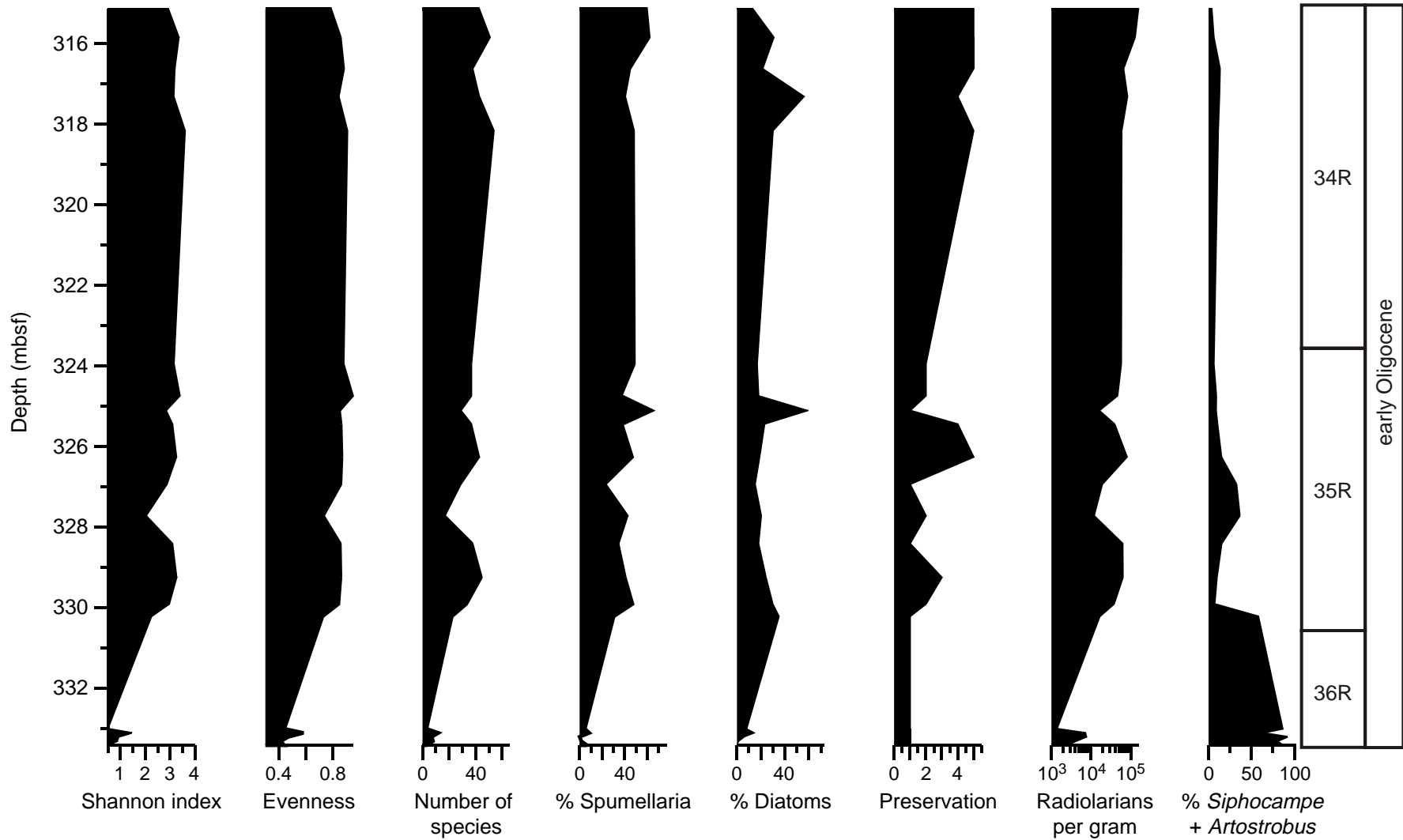


Table T1. General data for Leg 183 sites.

Site:	1138	1139	1140
Geography (Fig. F1, p. 22):	Central Kerguelen Plateau, 180 km east-southeast of Heard Island	350 km west-southwest of the Kerguelen archipelago, Skiff Bank (Leclaire Rise)	Northernmost Kerguelen Plateau, 270 km north of the Kerguelen archipelago
Core depth (mbsf):	842.7	694.2	321.9
Water depth (m):	1141	1415	2394
Basement:	Basalts overlain by volcanoclastic rock layers were recovered below 689 mbsf from the lower 144 m of the hole; age: Late Cretaceous	Altered volcanoclastic rocks, basalts, and one minor sedimentary bed from the lower 233 m of the hole; age: late Eocene?	Pillow basalts on three minor sediment beds from the lower 87.38 m of the hole; age: late Eocene–early Oligocene
Sediments recovered down to (mbsf):	689	461	234
Sedimentology:	655-m pelagic ooze, chalk, and calcareous claystone overlying 43 m of glauconitic calcareous sandstone and silty clay interbedded with sandstone and conglomerate	383-m calcareous claystone and chalk with thin intervals of calcareous ooze and chalk at the top and base overlying a <10-m interval of sandy packstone and 77-m grainstone	Pelagic ooze and chalk, whole sedimentary section
Eocene/Oligocene (Fig. F2, p. 23):	Base of Core 183-1138A-36R	Sections 183-1139A-38R-2 to 41R-1	Cores 183-1140A-37R to 26R

Note: All data are from Shipboard Scientific Party (2000) except Eocene/Oligocene data for Holes 1138A and 1139A.

Table T2 (continued).

Subepoch	Core, section, interval (cm)	Depth (mbsf)	Abundance	Preservation	Litheliidae					Spongodiscidae					Sponguridae										
					<i>Lithelius</i> sp. A gr.	<i>Lithelius</i> sp. B	<i>Lithelius</i> sp. C	<i>Lithelius</i> sp. D	<i>Lithelius</i> sp. E	<i>Prunopyle?</i> <i>hayesi</i>	<i>Prunopyle?</i> <i>trypopyrena</i>	<i>Prunopyle?</i> <i>polyacantha</i> gr.	<i>Prunopyle?</i> <i>fragilis</i>	<i>Prunopyle?</i> cf. <i>titan</i>	<i>Prunopyle?</i> sp. A	<i>Prunopyle?</i> sp. B	<i>Prunopyle?</i> sp. C gr.	<i>Spongodiscus</i> sp. aff. <i>Spongodiscus maculatus</i>	<i>Spongopyle</i> <i>osculosa</i>	<i>Perichlamydidium</i> <i>limbatum</i>	<i>Spongopyle</i> sp. A	<i>Stylodictya</i> <i>ocellata?</i>	<i>Stylodictya</i> <i>aculeata</i>	<i>Stylodictya</i> <i>validispina</i>	<i>Amphymenium</i> <i>splendiarmatum</i>
early Oligocene	183-1138A-																								
	34R-1, 103-105	315.14	A	G	50	32	32																		
	34R-2, 23-25	315.84	A	G	27	21	23	16		1	16	4		3										3	1
	34R-2, 101-103	316.62	A	G	17	12	14	29																2	1
	34R-3, 20-22	317.31	A	M	9	2	23	27																	
	34R-3, 105-107	318.16	A	G	32		12	15	22																
	35R-1, 24-026	323.95	R	P	27		22	14	26																
	35R-1, 103-105	324.74	R	P	27		9	12	9	1			20												
	35R-1, 140-142	325.11	C-R	P	14		23	4	8	2				1											
	35R-2, 24-26	325.45	A-C	G	42		4	8	12																
	35R-2, 105-107	326.26	C	G	26	18	34		47															4	1
	35R-3, 23-025	326.94	C-R	P	17				9																
	35R-3, 101-103	327.72	R	M	42		42																		
	35R-4, 20-022	328.41	C	P	35		9		22			4												8	
	35R-4, 104-106	329.25	C	M	57	15	39	11	32															1	
	35R-5, 20-022	329.91	C	P	52	7	47		8															4	
	35R-5, 51-53	330.22	R	P	3	4	7		7															2	
	36R-1, 0-2	333.01	R	P																					
	36R-1, 10-12	333.11	R	P	8		1		1																
	36R-1, 20-22	333.21	R	P																					
36R-1, 31-33	333.32	R	P	1																					
36R-1, 41-43	333.42	R	P	1																					

Table T2 (continued).

Subepoch	Core, section, interval (cm)	Depth (mbsf)	Abundance	Preservation	Plagiacanthidae														Pterocorythidae								
					<i>Lithomelissa dupliphysa</i>	<i>Pterosyringium hamata</i>	<i>Lithomelissa gelasinus</i>	<i>Lithomelissa</i> sp. aff. <i>Lithomelissa ehlenbergi</i>	<i>Lithomelissa?</i> sp. A	<i>Antarctissa longa</i>	<i>Antarctissa robusta</i>	<i>Antarctissa</i> sp. cf. <i>A. conradae</i>	<i>Antarctissa?</i> sp. A	<i>Antarctissa?</i> sp. B	<i>Antarctissa</i> sp. C gr.	<i>Antarctissa</i> sp. D	<i>Antarctissa</i> spp. gr.	<i>Peridium?</i> sp. A	<i>Peridium?</i> sp. B	<i>Nassellaria</i> fam. gen. sp. indet I	<i>Ceratocyrtis stigi</i>	<i>Ceratocyrtis</i> sp. aff. <i>Ceratocyrtis stigi</i>	<i>Ceratocyrtis robustus</i> gr.	<i>Ceratocyrtis mashae</i>	<i>Lophophaena capito</i>	<i>Carpocanarium</i> sp. A	<i>Lamprocydas</i> sp. A
early Oligocene	183-1138A-																										
	34R-1, 103–105	315.14	A	G	1	1																					
	34R-2, 23–25	315.84	A	G	4	23																					
	34R-2, 101–103	316.62	A	G	13	6	8																				
	34R-3, 20–22	317.31	A	M	4	4	13																				
	34R-3, 105–107	318.16	A	G			2	1																			
	35R-1, 24–026	323.95	R	P																							
	35R-1, 103–105	324.74	R	P																							
	35R-1, 140–142	325.11	C-R	P																							
	35R-2, 24–26	325.45	A-C	G			3	1																			
	35R-2, 105–107	326.26	C	G																							
	35R-3, 23–025	326.94	C-R	P																							
	35R-3, 101–103	327.72	R	M																							
	35R-4, 20–022	328.41	C	P																							
	35R-4, 104–106	329.25	C	M				2																			
	35R-5, 20–022	329.91	C	P																							
	35R-5, 51–53	330.22	R	P																							
	36R-1, 0–2	333.01	R	P																							
	36R-1, 10–12	333.11	R	P																							
	36R-1, 20–22	333.21	R	P																							
	36R-1, 31–33	333.32	R	P																							
	36R-1, 41–43	333.42	R	P																							

Table T2 (continued).

Subepoch	Core, section, interval (cm)	Depth (mbsf)	Abundance	Preservation	Artostrobiidae																		
					<i>Spirocyrtis greeni</i>	<i>Botryostrobos kerguelensis</i>	<i>Artostrobos pretabulatus</i>	<i>Artostrobos pusillum</i> gr.	<i>Siphocampe nodosaria</i>	<i>Siphocampe arachnea</i> gr.	<i>Siphocampe acephala</i> gr.	<i>Siphocampe? elizabethae</i>	<i>Artostrobos stathmeporoides</i>	<i>Siphocampe</i> sp. A	<i>Siphocampe</i> sp. B	<i>Siphocampe</i> sp. C	<i>Siphocampe</i> sp. D	<i>Siphocampe</i> sp. E	<i>Siphocampe</i> sp. F	<i>Dictyoprora physothorax</i>	<i>Dictyoprora</i> sp. A	<i>Plannapus hornibrooki</i>	<i>Plannapus mauricei</i>
early Oligocene	183-1138A-																						
	34R-1, 103-105	315.14	A	G				17															3
	34R-2, 23-25	315.84	A	G			10	8	1	17													7
	34R-2, 101-103	316.62	A	G	1	3	3	17	17	14													6
	34R-3, 20-22	317.31	A	M						24	10												7
	34R-3, 105-107	318.16	A	G			9	22		2	22		1	4									3
	35R-1, 24-026	323.95	R	P			13	17															12
	35R-1, 103-105	324.74	R	P			32	18	4														17
	35R-1, 140-142	325.11	C-R	P				9			2	4											9
	35R-2, 24-26	325.45	A-C	G					19	13	16												25
	35R-2, 105-107	326.26	C	G			22	37	12	18	10		2										19
	35R-3, 23-025	326.94	C-R	P	1			55	22	8	25		4	2									22
	35R-3, 101-103	327.72	R	M				82		1	4												7
	35R-4, 20-022	328.41	C	P			17	38	1	18	22												1
	35R-4, 104-106	329.25	C	M			28	32	7		12												14
	35R-5, 20-022	329.91	C	P		2		27															12
	35R-5, 51-53	330.22	R	P				96	22	6	14												12
	36R-1, 0-2	333.01	R	P				19															
	36R-1, 10-12	333.11	R	P				78			3												
	36R-1, 20-22	333.21	R	P				69	3		2	2											
36R-1, 31-33	333.32	R	P				52			1													
36R-1, 41-43	333.42	R	P				13																

Table T3. Summary of radiolarian faunal indices, Hole 1138A.

Core, section, interval (cm)	Depth (mbsf)	Species (N)	Individuals (N)	Margalef index	Shannon index	Evenness	Spumellarians* (%)	Diatoms† (%)	Preservation	<i>Siphocampe</i> (%)	Radiolarians per gram
183-1138A-											
34R-1, 103-105	315.14	42	490	6.62	2.92	0.78	59.02	13.58	G	3.61	153,891
34R-2, 23-25	315.84	50	430	8.08	3.34	0.85	61.41	30.99	G	6.07	127,942
34R-2, 101-103	316.62	37	363	6.11	3.17	0.88	44.25	21.62	G	13.22	64,859
34R-3, 20-22	317.31	42	516	6.56	3.13	0.84	39.63	56.38	M-G	12.40	81,898
34R-3, 105-107	318.16	53	488	8.40	3.59	0.90	47.42	30.22	G	11.13	58,786
35R-1, 24-26	323.95	36	402	5.84	3.13	0.87	48.26	17.11	P-M	5.97	57,118
35R-1, 103-105	324.74	36	353	5.97	3.38	0.94	36.54	18.29	P-M	8.78	46,246
35R-1, 140-142	325.11	28	198	5.11	2.82	0.85	63.78	59.50	P	8.67	15,875
35R-2, 24-26	325.45	36	372	5.91	3.08	0.86	37.33	23.29	M-G	10.31	39,039
35R-2, 105-107	326.26	42	535	6.53	3.23	0.87	46.62	19.10	G	14.90	79,855
35R-3, 23-25	326.94	28	345	4.62	2.86	0.86	22.26	15.33	P	32.34	18,894
35R-3, 101-103	327.72	16	238	2.74	2.02	0.73	41.77	20.47	P-M	36.29	11,708
35R-4, 20-22	328.41	37	421	5.96	3.08	0.85	33.75	18.26	P	15.14	62,517
35R-4, 104-106	329.25	44	610	6.70	3.25	0.86	40.16	24.41	M	9.67	62,604
35R-5, 20-22	329.91	33	385	5.38	2.95	0.84	47.01	30.13	P-M	7.01	37,388
35R-5, 51-53	330.22	22	254	3.79	2.24	0.72	30.24	35.25	P	58.06	16,554
36R-1, 0-2	333.01	3	22	0.65	0.49	0.44	4.55	8.33	P	86.36	1,371
36R-1, 10-12	333.111	12	128	2.27	1.45	0.58	8.59	14.67	P	63.28	7,131
36R-1, 20-22	333.21	7	89	1.34	0.92	0.47	0.00	6.32	P	92.13	7,528
36R-1, 31-33	333.32	8	66	1.67	0.86	0.42	1.52	1.50	P	80.30	4,123
36R-1, 41-43	333.42	3	15	0.74	0.49	0.44	6.67	0.00	P	86.67	2,447

Notes: Preservation: P = poor, M = Moderate, G = Good. * = percentage relative to nassellarians. † = Percentage relative to total radiolarians. N = Number. Diversity and evenness measures are defined in text.

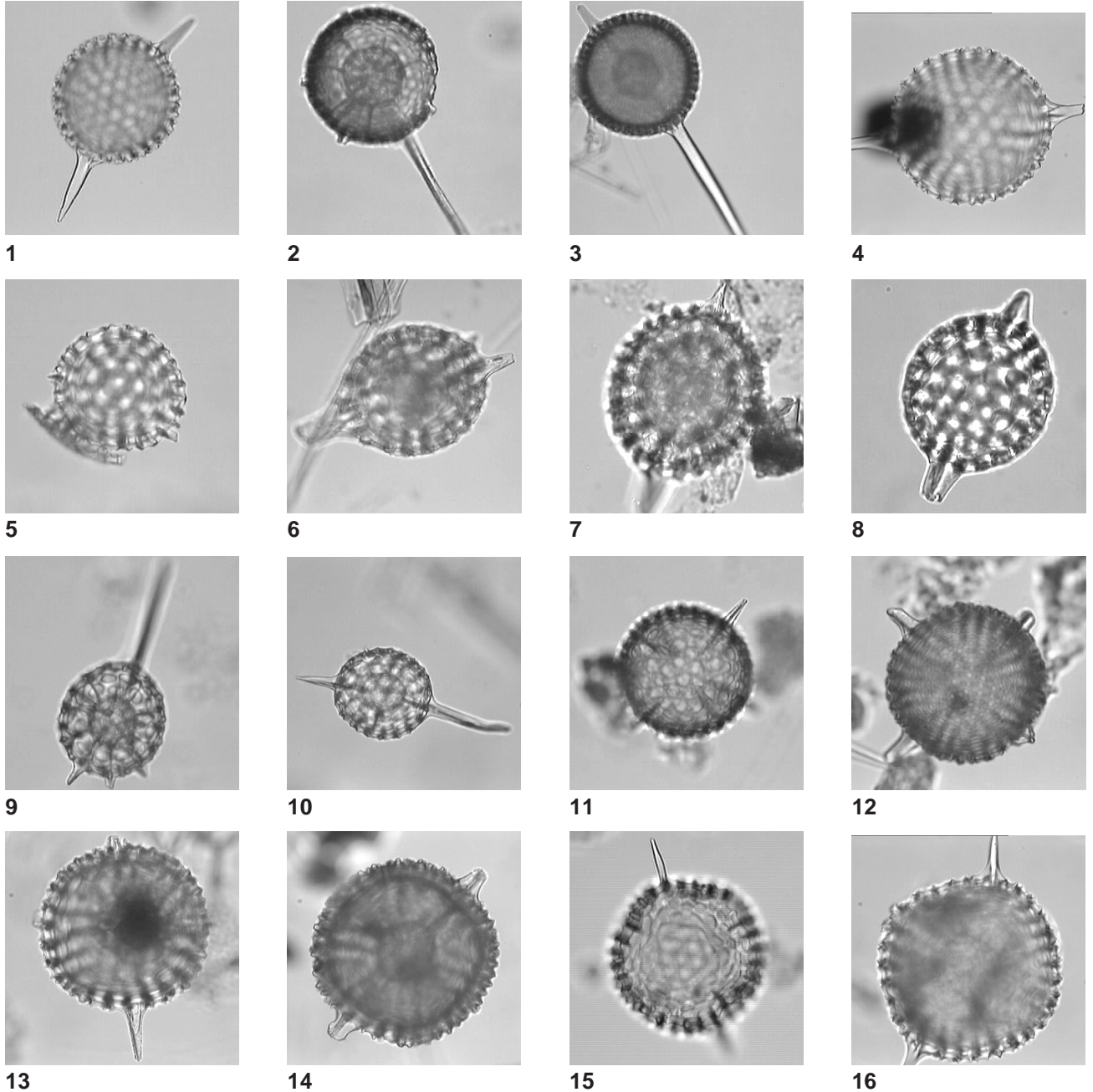
Table T4. Mean preservation of Eocene–Oligocene radiolarian faunas from Southern Ocean sites.

	Leg 120 Kerguelen Plateau		Leg 119 Kerguelen Plateau		Leg 71 Falkland Plateau		Leg 28 Ross Sea to Australia			Leg 183 Kerguelen Plateau
Time slice	748B*	749B*	738B†	744A†	511‡	512‡	274**	267**	264**	1138A
late Oligocene	2.6	2		3				2.2		
early Oligocene	2.5	2	1.8	3	2.6		2.3			1.8
late Eocene	1.5	1.5	1.8	1	2.5				1.4	1
middle Eocene	1.6	1.5	1.6	1	1.0	2.9			1.4	1

Notes: Evaluations of preservation were taken from all samples of the reported data, transformed into numerical values, and averaged for the time intervals indicated. 1 = preservation poor or no radiolarians preserved, 2 = preservation moderate, 3 = preservation good. Sources: * = Takemura (1992), † = Caulet (1991), ‡ = Weaver (1983), ** = Chen (1975).

Plate P1. Oligocene Actinommidae from the Kerguelen Plateau, Site 1138. 1. *Amphisphaera* sp. A; Sample 183-1138A-36R-1, 10–12 cm. 2. *Amphistylus*? sp. A; Sample 183-1138A-34R-2, 101–103 cm. 3. *Amphistylus angelinus* (Clark and Campbell); Sample 183-1138A-34R-3, 20–22 cm. 4. *Stylatractus* sp. A; Sample 183-1138A-36R-1, 10–12 cm. 5. *Stylatractus* sp. B; Sample 183-1138A-36R-1, 10–12 cm. 6–8. *Stylosphaera radiosa* Ehrenberg gr.; Sample 183-1138A-36R-1, 41–43 cm. 9–10. *Stylosphaera* sp. A gr.; Sample 183-1138A-34R-1, 103–105 cm. 11. *Hexacontium* sp. A; Sample 183-1138A-34R-1, 103–105 cm. 12. *Hexacontium* sp. B; Sample 183-1138A-34R-1, 103–105 cm. 13. *Axoprunum bispiculum* (Popofsky); Sample 183-1138A-34R-1, 103–105 cm. 14. *Axoprunum pierinae* (Clark and Campbell); Sample 183-1138A-34R-1, 103–105 cm. 15–16. *Axoprunum irregularis* Takemura; Samples 183-1138A-35R-4, 20–22 cm, and 34R-2, 23–25 cm.

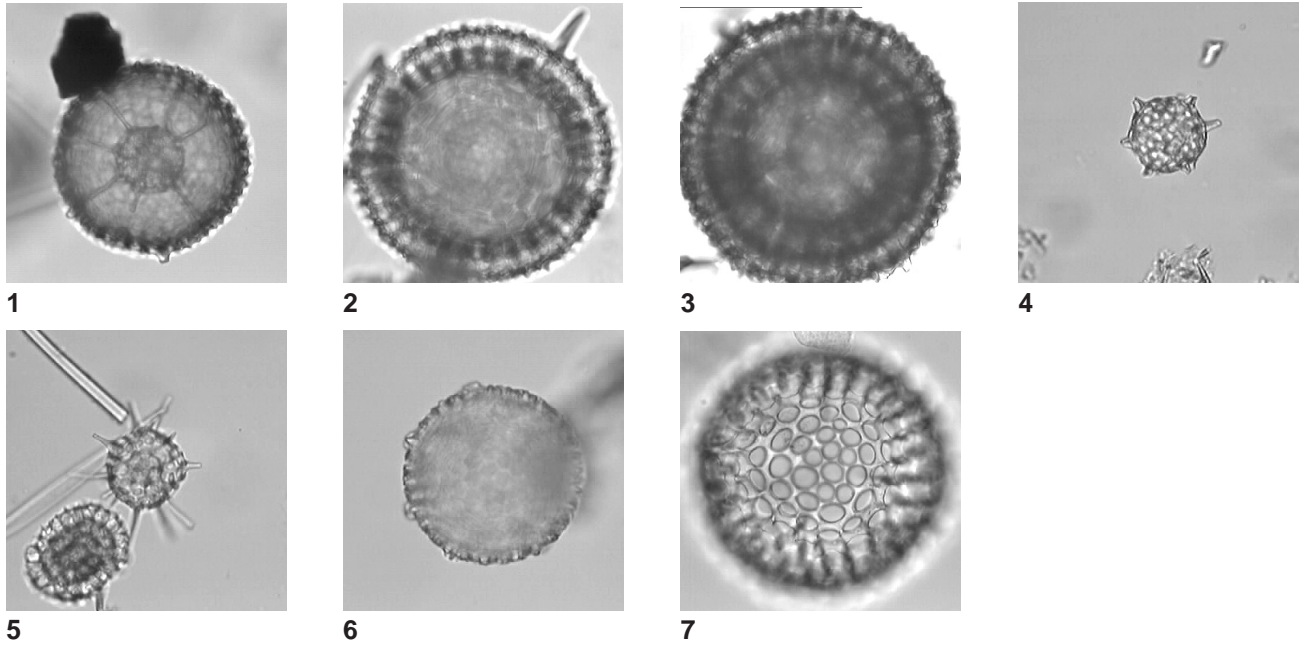
Family: Actinommidae



100 μ m

Plate P2. Oligocene Actinommidae and Pyloniidae from the Kerguelen Plateau, Site 1138. 1. *Actinomma henningsmoeni* Goll and Bjørklund; Sample 183-1138A-34R-3, 20–22 cm. 2–3. *Actinomma holtedahli* Bjørklund gr.; Sample 183-1138A-34R-1, 103–105 cm. 4–5. *Drymyomma? elegans* Jørgensen gr.; Sample 183-1138A-35R-1, 140–142 cm. 6–7. *Cenosphaera* sp. A gr.; Sample 183-1138A-35R-4, 104–106 cm. 8. Pylonid sp. 1; Sample 183-1138A-36R-1, 31–33 cm. 9. Pylonid sp. 2; Sample 183-1138A-34R-3, 20–22 cm. 10. Pylonid sp. 3; Sample 183-1138A-35R-5, 20–22 cm. 11. Pylonid sp. 4; Sample 183-1138A-35R-4, 104–106 cm. 12. Pylonid sp. 5; Sample 183-1138A-35R-1, 24–26 cm. 13. Pylonid sp. 6; Sample 183-1138A-35R-2, 24–26 cm.

Family: Actinommidae



Family: Pyloniidae

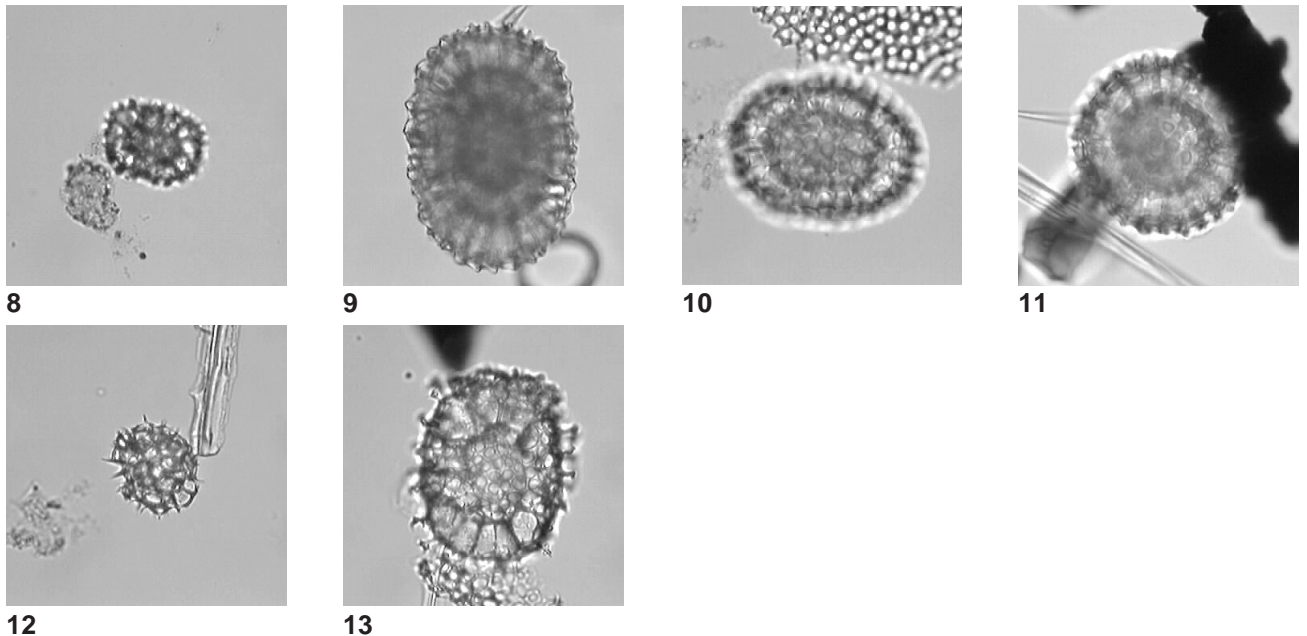
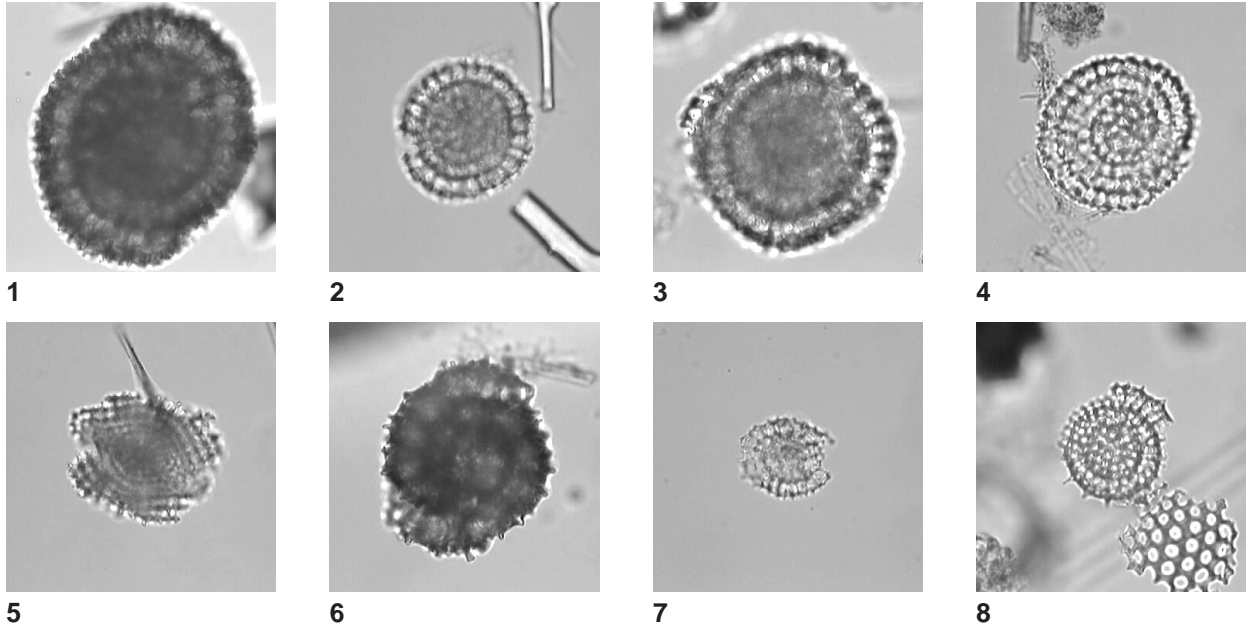
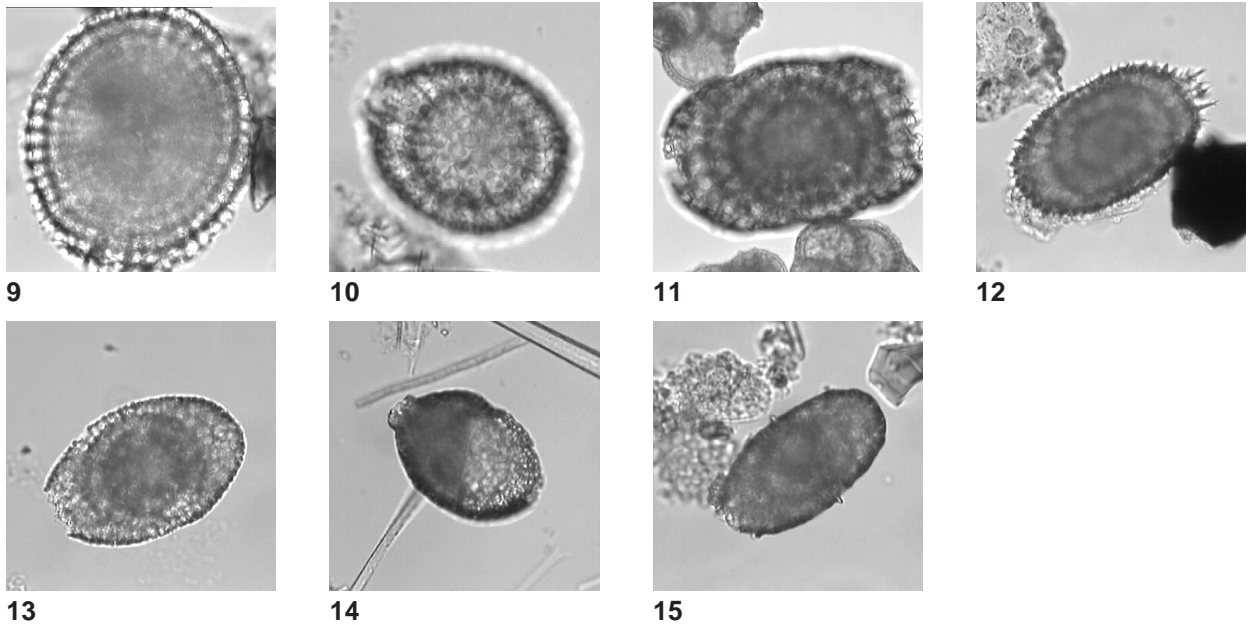


Plate P3. Oligocene Litheliidae from the Kerguelen Plateau, Site 1138. 1–4. *Lithelius* sp. A gr.; Sample 183-1138A-35R-2, 105–107 cm. 5. *Lithelius* sp. B; Sample 183-1138A-34R-3, 20–22 cm. 6. *Lithelius* sp. C; Sample 183-1138A-35R-2, 105–107 cm. 7. *Lithelius* sp. D; Sample 183-1138A-35R-2, 24–26 cm. 8. *Lithelius* sp. E; Sample 183-1138A-35R-2, 105–107 cm. 9. *Prunopyle?* *hayesi* Chen; Sample 183-1138A-35R-1, 103–105 cm. 10. *Prunopyle?* *trypopyrena* Caulet; Sample 183-1138A-34R-2, 23–25 cm. 11–12. *Prunopyle?* *polyacantha* Clark and Campbell gr.; Sample 183-1138A-34R-3, 105–107 cm. 13. *Prunopyle?* *fragilis* (Stöhr); Sample 183-1138A-35R-2, 24–26 cm. 14. *Prunopyle?* *titan* Clark and Campbell; Sample 183-1138A-34R-1, 103–105 cm. 15. *Prunopyle?* sp. A; Sample 183-1138A-35R-1, 140–142 cm.

Family: Litheliidae



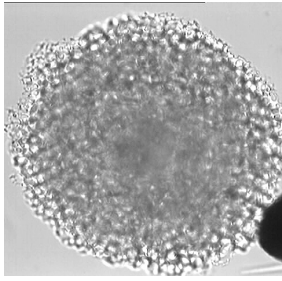
Family: Litheliidae



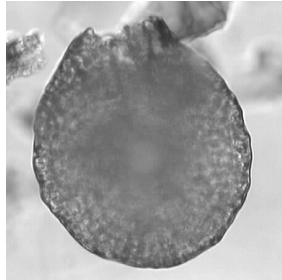
100 μm

Plate P4. Oligocene Spongodiscidae and Sponguridae from the Kerguelen Plateau, Site 1138. 1. *Spongodiscus* sp. aff. *Spongodiscus maculatus* Clark and Campbell; Sample 183-1138A-35R-3, 23–25 cm. 2. *Spongopyle osculosa* Dreyer; Sample 183-1138A-34R-2, 101–103 cm. 3. *Perichlamyidium limbatum* Ehrenberg; Sample 183-1138A-34R-2, 23–25 cm. 4. *Spongopyle* sp. A; Sample 183-1138A-35R-1, 140–142 cm. 5. *Stylodictya ocellata*? Ehrenberg; Sample 183-1138A-35R-4, 104–106 cm. 6. *Stylodictya aculeata* Jørgensen; Sample 183-1138A-35R-4, 104–106 cm. 7. *Stylodictya validispina* Jørgensen; Sample 183-1138A-34R-2, 23–25 cm. 8. *Amphymenium splendiararmatum* Clark and Campbell; Sample 183-1138A-35R-1, 103–105 cm. 9. *Amphycraspedum proxillum*? Sanfilippo and Riedel; Sample 183-1138A-35R-2, 105–107 cm.

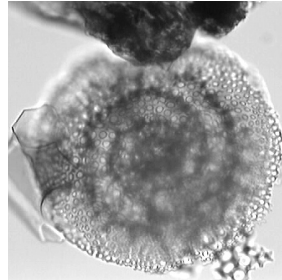
Family: Spongodiscidae



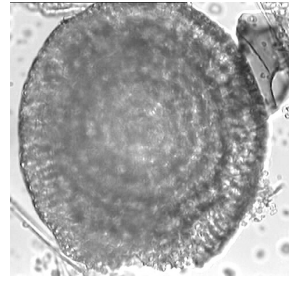
1



2



3

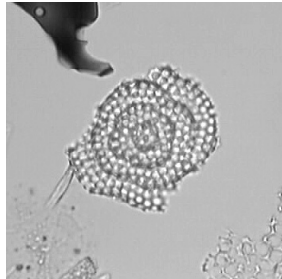


4

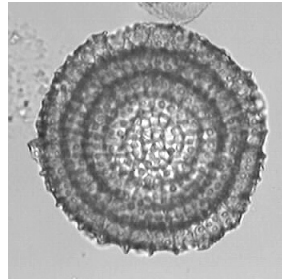
Family: Spongodiscidae



5

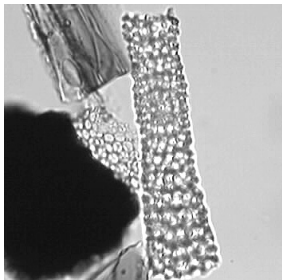


6

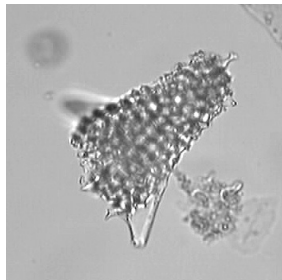


7

Family: Sponguridae



8



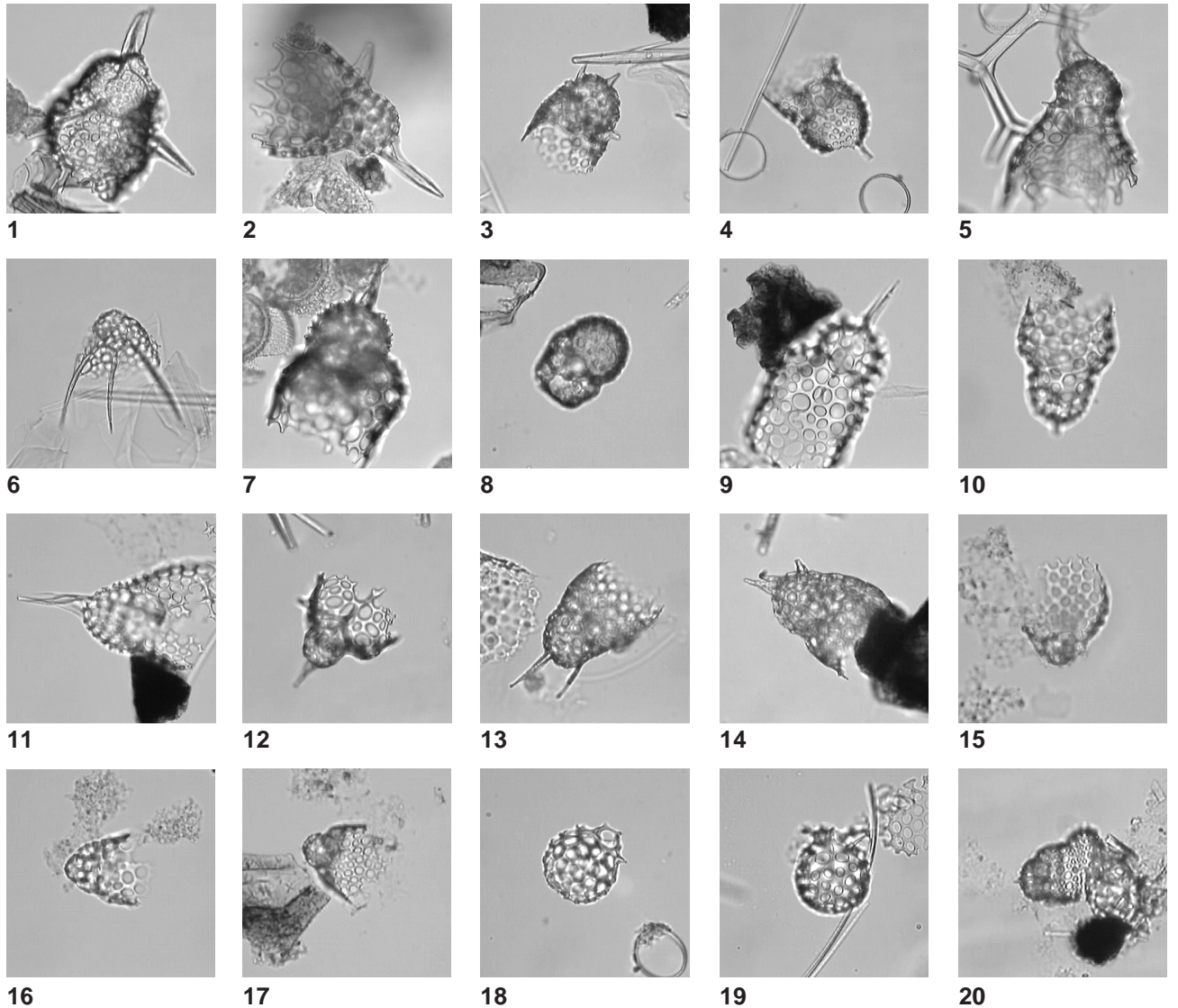
9



100 μ m

Plate P5. Oligocene Plagiacanthidae from the Kerguelen Plateau, Site 1138. 1. *Lithomelissa dupliphysa* Caulet; Sample 183-1138A-34R-3, 105–107 cm. 2. *Pterosyringium hamata* O'Connor; Sample 183-1138A-34R-2, 23–25 cm. 3. *Lithomelissa tricornis* Chen; Sample 183-1138A-34R-1, 103–105 cm. 4. *Lithomelissa gelasinus* O'Connor; Sample 183-1138A-34R-3, 20–22 cm. 5. *Lithomelissa* sp. aff. *L. ehrenbergi* Bütschli; Sample 183-1138A-35R-5, 20–22 cm. 6. *Lithomelissa?* sp. A; Sample 183-1138A-35R-1, 24–26 cm. 7. *Antarctissa longa* Petrushevskaya; Sample 183-1138A-34R-3, 105–107 cm. 8. *Antarctissa robusta* Petrushevskaya; Sample 183-1138A-34R-1, 103–105 cm. 9–10. *Antarctissa* sp. cf. *A. conradae* Chen; Sample 183-1138A-35R-4, 20–22 cm. 11. *Antarctissa?* sp. A; Sample 183-1138A-35R-5, 20–22 cm. 12. *Antarctissa?* sp. B; Sample 183-1138A-35R-1, 51–53 cm. 13–14. *Antarctissa* sp. C gr.; Samples 183-1138A-35R-2, 24–26 cm. 15–17. *Antarctissa?* spp. gr.; Sample 183-1138A-35R-5, 51–53 cm. 18. *Peridium?* sp. A; Sample 183-1138A-35R-3, 23–25 cm. 19. *Peridium?* sp. B; Sample 183-1138A-35R-2, 24–26 cm. 20. Nassellaria Gen. et sp. indet. I; Sample 183-1138A-35R-1, 140–142 cm.

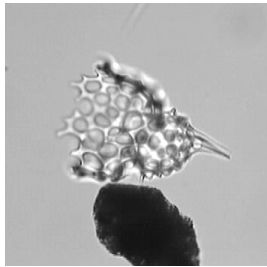
Family: Plagiacanthidae



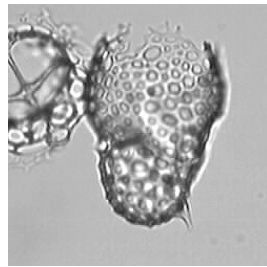
100 µm

Plate P6. Oligocene Plagiacanthidae, Pterocorythidae, Plagonidae, Cannobotridae, and Theoperidae from the Kerguelen Plateau, Site 1138. 1. *Ceratocyrtis stigi* (Bjørklund); Sample 183-1138A-35R-5, 20–22 cm. 2. *Ceratocyrtis* sp. aff. *C. stigi* (Bjørklund); Sample 183-1138A-35R-2, 105–107 cm. 3–4. *Ceratocyrtis robustus?* Bjørklund; Sample 183-1138A-35R-5, 20–22 cm. 5. *Ceratocyrtis mashae* Bjørklund; Sample 183-1138A-34R-1, 103–105 cm. 6. *Lophophaena capito* Ehrenberg; Sample 183-1138A-35R-2, 105–107 cm. 7. *Carpocanariu* sp. A; Sample 183-1138A-35R-1, 103–105 cm. 8. *Lamprocyclas* sp. A; Sample 183-1138A-35R-2, 24–26 cm. 9. *Tripodiscinus clavipes* Clark and Campbell; Sample 183-1138A-34R-2, 101–103 cm. 10. *Tripodiscinus* sp. A; Sample 183-1138A-35R-2, 105–107 cm. 11. *Botryocella pauciperforata* O'Connor; Sample 183-1138A-35R-4, 104–106 cm. 12. *Botryocella?* sp. A; Sample 183-1138A-34R-1, 103–105 cm. 13–15. *Cornutella profunda* Ehrenberg gr.; Sample 183-1138A-35R-5, 51–53 cm.

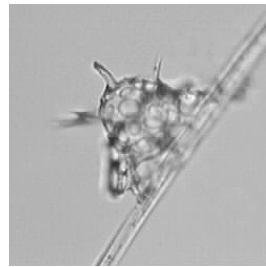
Family: Plagiacanthidae & Pterocorythidae (8)



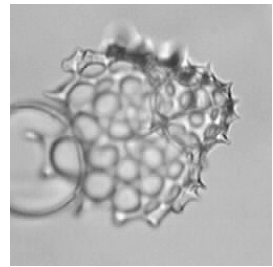
1



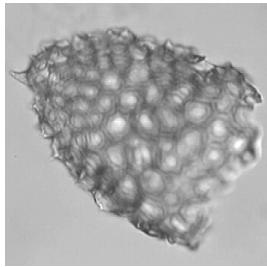
2



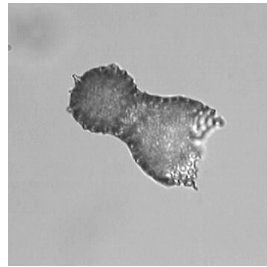
3



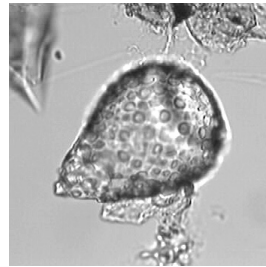
4



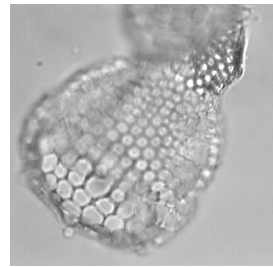
5



6

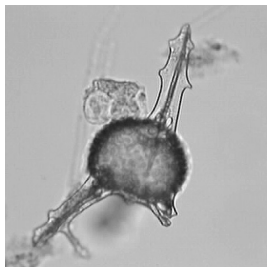


7

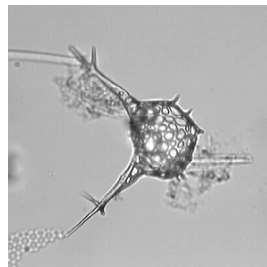


8

Family: Plagonidae

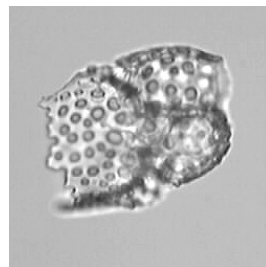


9

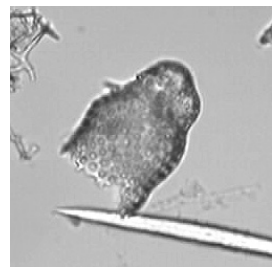


10

Family: Cannobotridae

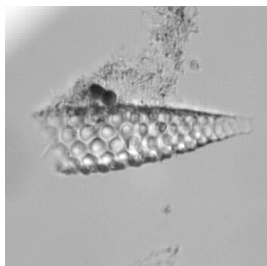


11

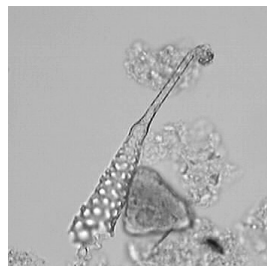


12

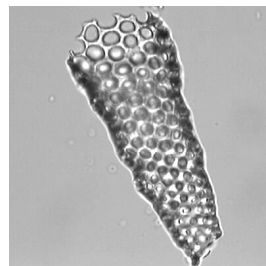
Family: Theoperidae



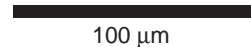
13



14



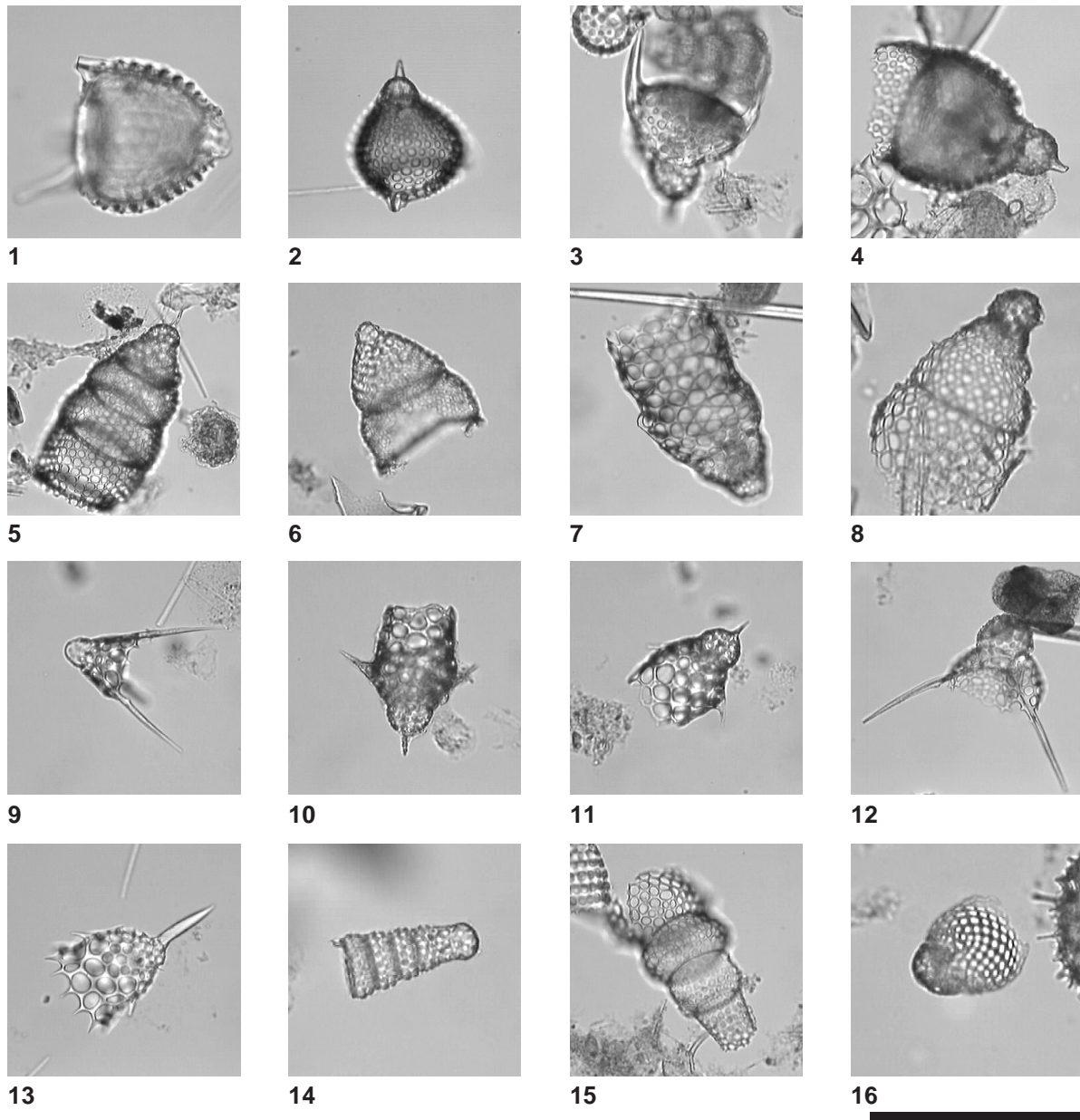
15



100 μ m

Plate P7. Oligocene Theoperidae from the Kerguelen Plateau, Site 1138. 1. *Lychnocanoma conica* (Clark and Campbell); Sample 183-1138A-35R-4, 20–22 cm. 2. *Lychnocanoma* sp. cf. *Lychnocanoma babylonis* (Clark and Campbell); Sample 183-1138A-34R-3, 20–22 cm. 3. *Lychnocanoma tripodium* (Ehrenberg); Sample 183-1138A-34R-3, 105–107 cm. 4. *Thyrsocyrtis*? sp.; Sample 183-1138A-34R-2, 23–25 cm. 5. *Eucyrtidium spinosum* Takemura; Sample 183-1138A-35R-1, 103–105 cm. 6. *Eucyrtidium punctatum* (Ehrenberg); Sample 183-1138A-35R-2, 105–107 cm. 7. *Eucyrtidium* sp. A; Sample 183-1138A-34R-3, 105–107 cm. 8. *Lophocyrtis* (*Apoplanius*) *klydus*? Sanfilippo and Caulet; Sample 183-1138A-34R-1, 103–105 cm. 9. *Dictyophimus craticula* Ehrenberg; Sample 183-1138A-35R-2 105–107 cm. 10. *Dictyophimus archipilium* Petrushevskaya; Sample 183-1138A-35R-2, 105–107 cm. 11. *Dictyophimus* sp. aff. *D. archipilium* Petrushevskaya; Sample 183-1138A-35R-2, 105–107 cm. 12. *Pseudodictyophimus gracilipes* Bailey gr.; Sample 183-1138A-34R-3, 105–107 cm. 13. *Eurystomoskevos petrushevskaae* Caulet; Sample 183-1138A-35R-5, 20–22 cm. 14. *Cyrtolagena laguncula* Haeckel; Sample 183-1138A-35R-5, 51–53 cm. 15. *Cyrtolagena* sp. A; Sample 183-1138A-34R-2, 101–103 cm. 16. Nassellaria Gen. et sp. indet. II; Sample 183-1138A-34R-2, 23–25 cm.

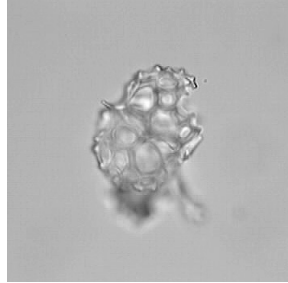
Family: Theoperidae



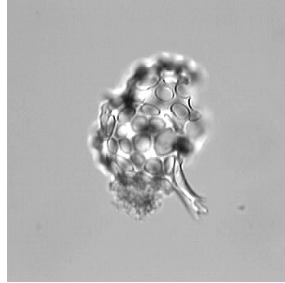
100 µm

Plate P8. Oligocene Acanthodesmiidae from the Kerguelen Plateau, Site 1138. 1–4. *Corythospyris fiscella* Goll gr.; Sample 183-1138A-36R-1, 20–22 cm. 5. *Corythospyris jubata* Goll; Sample 183-1138A-35R-5, 20–22 cm. 6. *Dendrospyris* sp. A; Sample 183-1138A-35R-4, 20–22 cm. 7. *Dendrospyris stabilis* Goll; Sample 183-1138A-35R-2, 24–26 cm. 8. *D. stabilis* Goll (bottom and top view); Sample 183-1138A-36R-1, 31–33 cm.

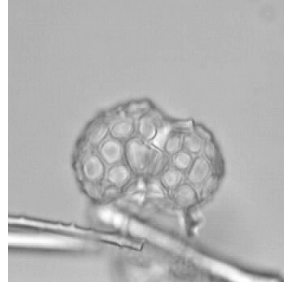
Family: Acanthodesmiidae



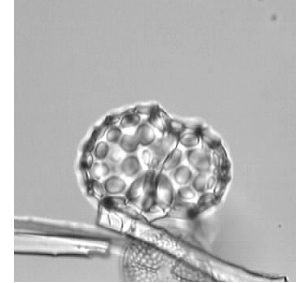
1a



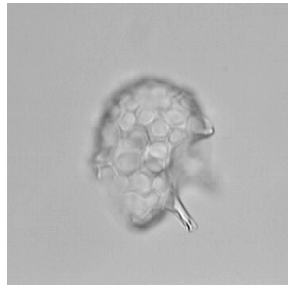
1b



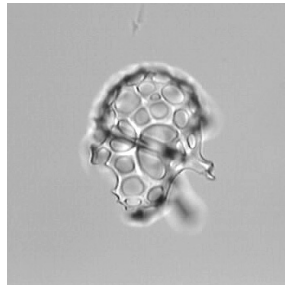
2a



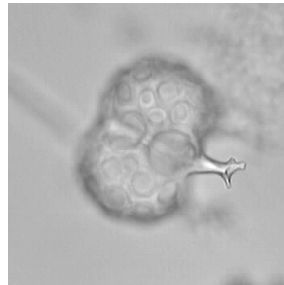
2b



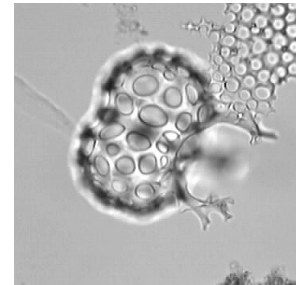
3a



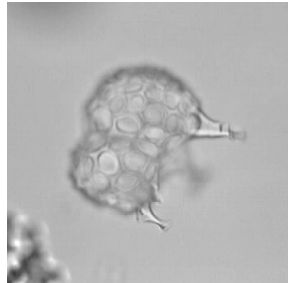
3b



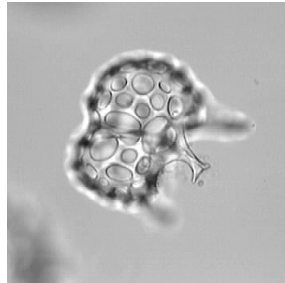
4a



4b



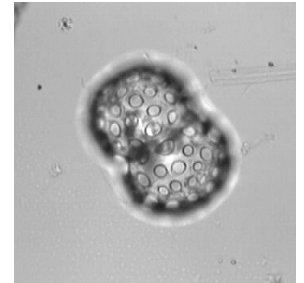
5a



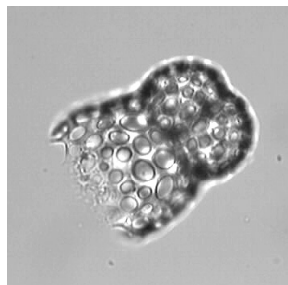
5b



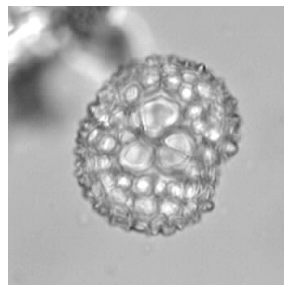
6a



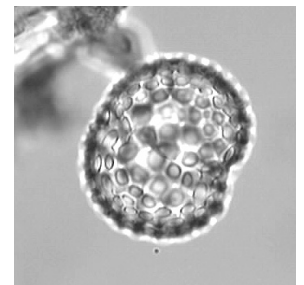
6b



7



8a



8b

100 μ m

Plate P9. Oligocene Artostrobiidae from the Kerguelen Plateau, Site 1138. 1. *Spirocyrtis greeni* O'Connor; Sample 183-1138A-35R-2, 105–107 cm. 2. *Botryostrobos kerguelensis*; Sample 183-1138A-35R-4, 104–106 cm. 3–4. *Artostrobos annulatus* (Bailey) gr.; Sample 183-1138A-34R-2, 101–103 cm. 5. *Artostrobos pretabulatus* Petrushevskaya; Sample 183-1138A-35R-4, 104–106 cm. 6–10. *Artostrobos pusillum* (Ehrenberg) gr.; Sample 183-1138A-35R-4, 104–106 cm. 11. *Siphocampe nodosaria* (Haeckel); Sample 183-1138A-35R-4, 104–106 cm. 12–13. *Siphocampe arachnea* (Ehrenberg) gr.; Sample 183-1138A-34R-2, 23–25 cm. 14–17. *Siphocampe acephala* (Ehrenberg) gr.; Sample 183-1138A-35R-2, 24–26 cm. 18. *Siphocampe? elizabethae* sensu Hollis; Sample 183-1138A-36R-1, 20–22 cm.

Family: Artostrobiidae

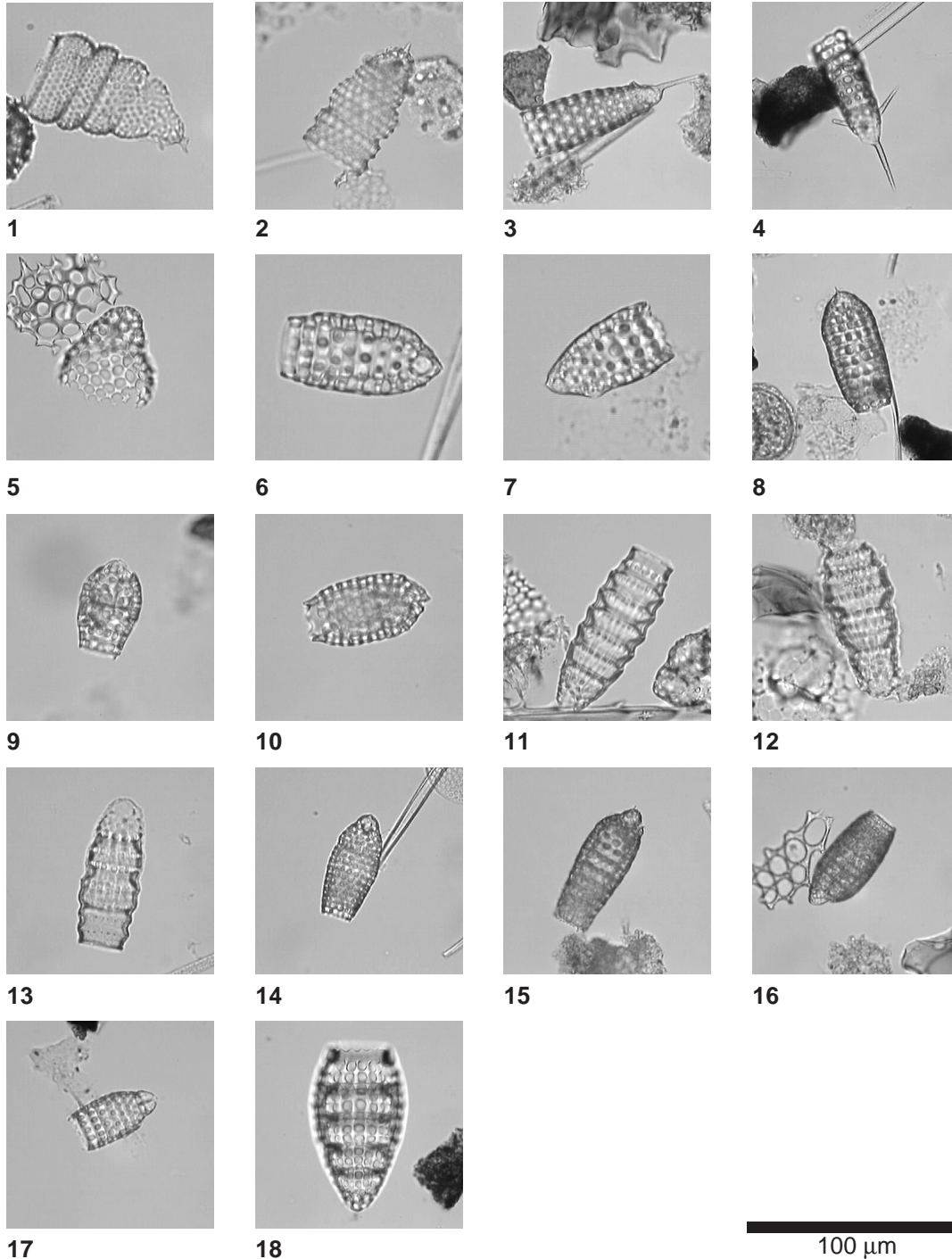
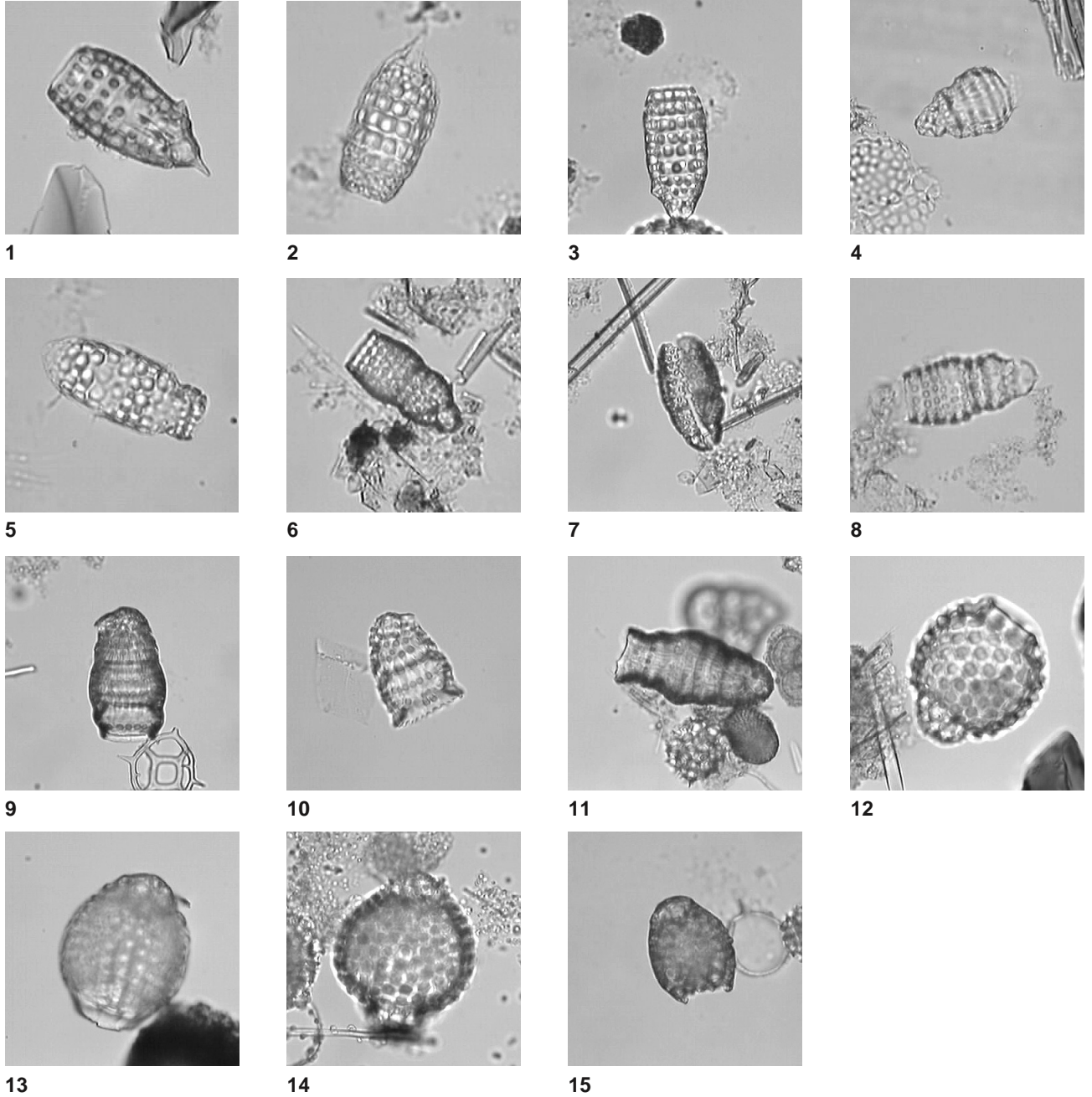


Plate P10. Oligocene Artostrobiidae from the Kerguelen Plateau, Site 1138. 1–2. *Artostrobus stathmeporoides*; Sample 183-1138A-35R-3, 23–25 cm. 3. *Siphocampe* sp. A; Sample 183-1138A-35R-3, 23–25 cm. 4. *Siphocampe* sp. B; Sample 183-1138A-35R-2, 24–26 cm. 5. *Siphocampe* sp. C; Sample 183-1138A-35R-2, 24–26 cm. 6. *Siphocampe* sp. D; Sample 183-1138A-35R-1, 140–142 cm. 7. *Siphocampe* sp. E; Sample 183-1138A-35R-1, 140–142 cm. 8. *Siphocampe* sp. F; Sample 183-1138A-35R-4, 104–106 cm. 9–10. *Dictyoprora physothorax* Cautlet; Sample 183-1138A-35R-2, 105–107 cm. 11. *Dictyoprora* sp. A; Sample 183-1138A-34R-3, 105–107 cm. 12. *Plannapus hornibrooki* O'Connor; Sample 183-1138A-34R-2, 23–25 cm. 13. *Plannapus mauricei* O'Connor; Sample 183-1138A-35R-4, 104–106 cm. 14. *Plannapus* sp. A; Sample 183-1138A-35R-3, 23–25 cm. 15. *Dicolocapsa* sp. A (Haeckel); Sample 183-1138A-34R-3, 20–22 cm.

Family: Artostrobiidae



100 μ m